
FACULTY OF TECHNOLOGY

# Biochar/Polyurethane composites: Mechanical and electrical properties

Mika Pitkänen

Process Engineering

Master's thesis

June 2019

# TIIVISTELMÄ OPINNÄYTETYÖSTÄ

Oulun yliopisto Teknillinen tiedekunta

| Koulutusohjelma (kandidaatintyö, diplomityö)<br>Prosessitekniikan koulutusohjelma | Pääaineopintojen ala (lisensiaatintyö) |
|---|---|
| Tekijä<br>Mika Pitkänen | Työn ohjaaja yliopistolla<br>Prof Kristiina Oksman, TkT Maiju Hietala |

Työn nimi

Polyuretaani/biohiili komposiitien mekaaniset ja sähköiset ominaisuudet

| Opintosuunta | Työn laji | Aika | Sivumäärä |
|---|---|---|---|
| Biotuotetekniikka | Diplomityö | 06/2019 | 82 |


Tiivistelmä

Rajalliset luonnonvarat, tiukentuvat lainsäädännöt sekä ympäristötietoisuuden lisääntyminen lisäävät kiinnostusta ympäristöystävällisten materiaalien käytöstä. Erityisesti vaihtoehtoja muovin ja komposiittien valmistuksessa käytetylle raakaöljylle etsitään kovasti. Mikäli raakaöljy halutaan korvata biopohjaisella raaka-aineella, tulee sen täyttää vaaditut ominaisuudet. On yleisesti tiedossa, että biopohjaisiin materiaaleihin ja lisäaineiden ominaisuuksiin vaikuttaa suuresti raaka-aineet ja prosessointi olosuhteet. Yksi mahdollinen vaihtoehto, jossa biopohjaisia täyteaineita voitaisiin käyttää, ovat sähköä johtavat biohiilikomposiitit. Sähköä johtavia polyuretaanikomposiitteja voidaan käyttää esimerkiksi sellaisissa teollisuuden käyttötarkoituksissa, jossa vaaditaan kulutuksenkestävyyttä. Tämä auttaisi vähentämään raakaöljypohjaisten täyteaineiden käyttöä tällä alalla. Biohiilen raaka-ainetta on yleisesti hyvin saatavilla joka puolella maailmaa.

Tämän työn päätavoitteena oli tutkia voiko polyuretaanista ja biohiilestä valmistaa sähköä johtavia komposiitteja. Toinen työn tavoite oli tutkia kuinka biohiili vaikuttaa polyuretaanin kulutuksen kestoon ja kovuuteen. Ensimmäinen osio tässä työssä on kirjallisuuskatsaus, jossa keskitytiin sähköä johtaviin komposiitteihin, sekä niissä käytettyihin täyteaineisiin. Kirjallisuusosiossa keskityttiin keräämään tietoa käytössä olevista hiili, ja biohiili täyteainesta sekä niiden ominaisuuksista. Työn kokeellisessa osiossa eri puulajeista valmistetut biohiilet jauhettiin 300-700nm partikkelikokoon, sekoitettiin polyuretaaniin ja valettiin polyuretaani-biohiilikomposiitti levyiksi. Valmistettujen komposiittien kulutuksen kestoa ja kovuutta, kuten myös sähköisiä ominaisuuksia tutkittiin mittaamalla dielektrisiä ominaisuuksia komposiiteista. Koska hyvän dispersion saaminen komposiittien valmistuksessa on haastavaa, tutkittiin komposiittien mikrorakennetta ja polyuretaanin/biohiilen vuorovaikutusta kenttäemissiopyyhkäisy-elektronimikroskoopilla.

Tulokset osoittavat, että tehdyillä polyuretaani/biohiili komposiiteilla on hyvät kulutuksenkesto ja kovuus ominaisuudet, nämä ominaisuudet huononivat vain hieman alkuperäisistä arvoista, mutta sähköistä perkolaatiota ei saavutettu edes korkeimmilla biohiilipitoisuuksilla (15 m%). Syynä huonoihin elektronisiin ominaisuuksiin on huonolaatuinen, sähköä johtamaton biohiili ja suuri huokoisuus. Nämä ominaisuudet johtuvat biohiilen valmistuksessa käytetystä lämpötilasta. Mikroskooppikuvat komposiittien rakenteesta osoittavat, että polyuretaanin ja biohiilen adheesio on hyvä mutta kaikissa komposiiteissa on suuri huokoisuus, joka vaikuttaa komposiittien ominaisuuksiin negatiivisesti. Tulevissa tutkimuksissa tulisi keskittyä biohiilen sähköisten ominaisuuksien parantamiseen sekä huokoisuuden estämiseen.


Muita tietoja

# ABSTRACT
# FOR THESIS

University of Oulu Faculty of Technology

| Degree Programme (Bachelor's Thesis, Master's Thesis) | Major Subject (Licentiate Thesis) |
|---|---|
| Process Engineering | |
| **Author** | **Thesis Supervisor** |
| Mika Pitkänen | Prof. Kristiina Oksman, Dr. Maiju Hietala |

Title of Thesis

Preparation of polyurethane/biochar composites and their mechanical and electrical properties

| Major Subject | Type of Thesis | Submission Date | Number of Pages |
|---|---|---|---|
| Bioproducts | Master's thesis | 06/2019 | 82 |


Abstract

As non-renewable resources are being depleted, legislative regulations are tightening and environmental awareness is increasing, the interest in using more environment-friendly materials is growing. In particular, there is higher demand for alternative options to petroleum-based materials, such as polymers and composites. However, in order to replace these materials with bio-based options, their quality should be the same as or better than petroleum-based materials. It is known that the properties of bio-based materials and additives are highly affected by the feedstock and its processing conditions. Biochar is a viable option for use as an additive in polymers to create electrically conductive polymer composites. For example, there is interest in developing conductive polyurethane composites to be used as an abrasion-resistant material in industry. The use of biochar would also decrease the amounts of petroleum-based additives used in the field. Moreover, the raw material options for biochar are abundant.

The main objective of this study was to study whether it is possible to prepare electrically conductive composite materials by incorporating biochar (BC) in polyurethane (PU). Another aim was to study how the addition of biochar would affect the wear and hardness properties of polyurethane. For the first part of the thesis, a literature survey was conducted focusing on electrically conductive polyurethane composites and the type of additives used in them. The focus was to gather information about the carbon and biochar additives used and their properties. In the experimental part, biochar based on different wood species was ground to smaller particle sizes (300-700 nm), and these biochar powders were mixed with polyurethane and then cast into sheets for further characterization. The dielectric, wear, and hardness properties of the prepared PU/BC composites were studied as well as the dispersion of the biochar in the polyurethane matrix and the interface between the biochar and PU.

The results show that PU-BC composites have good wear properties and hardness values, which were only slightly lower than those of neat PU. However, electrical percolation was not achieved even with the highest amounts of BC. Biochar had the greatest effect on the electrical properties as it was found to be non-conductive due to the low pyrolysis temperature as well as the high void content in the composites. The results show that biochar should be of higher quality to be able to conduct electrical current. Nevertheless, good adhesion between additive and matrix was achieved in the composites according to microscopy images. In future work, more focus should be placed on improving the electrical conductivity of biochar in order to achieve composites suitable for electrical applications.


Additional Information

# PREFACE

The work leading to this Master's thesis was mostly conducted in the Fibre and Particle Engineering research unit of the University of Oulu during the summer and autumn of 2018. Electrical testing was done in the Microelectronics research unit of the University of Oulu. Ravelast OY, Kello, Finland provided materials for polyurethanes and The biochars used in this study were provided by Noireco Oy, Mikkeli, Finland This thesis work was a part of a project called "Green Carbon Nanofibres for Large Area Electronics" (Grelectronics), funded by Business Finland.

I would like to thank Professor Mirja Illikainen for giving me the opportunity initially to start working in the Fibre and Particle Engineering research unit. Without this opportunity, this work would never have been realized. I would also like to thank all the people who have been involved in the process by giving me guidelines and important advice for this work. In no special order, these people include Petteri Piltonen, who helped with the chemistry side of this work; Tuukka Nissilä, who helped a lot with different computer programs; Jarno Karvonen, who was always ready to help with any practical problems in the laboratory; Jarkko Tolvanen, who made the electrical measurements of the composites; Pasi Juntunen, who introduced me to electron microscopy; Kaisu Ainassaari, who made the surface area measurements; Tiina Laitinen and Veli-Pekka Moilanen, who helped with the Raman analysis, and all the numerous other people whom I have worked with and the whole staff of the Fibre and Particle Engineering unit, who created a friendly and collaborative atmosphere in which it was easy to work

A special thank you goes to my supervisors, FiDiPro Professor Kristiina Oksman (Luleå University of Technology) and Maiju Hietala (Dr. Tech) from Oulu University, for their guidance and feedback during the whole working process. It has been really rewarding and great to have the opportunity to work with people who are so committed to research work.

Oulu 13.06.2019 Mika Pitkänen

# TABLE OF CONTENTS

# SYMBOLS AND ABBREVIATIONS

| | |
|---|---|
| BET | Brunauer-Emmet-Teller theory |
| CB | Carbon black |
| CEC | Cation exchange capacity |
| CNT | Carbon nanotubes |
| MW | Molecular weight |
| MWNT | Multiwall nanotubes |
| OH | Hydroxyl group |
| PEP | Polyester polyol |
| PETP | Polyether polyol |
| PU | Polyurethane |
| SWNT | Single wall nanotubes |
| vol% | Volume percentage |
| wt% | Weight percentage |

# 1 INTRODUCTION

The limited depletion of non-renewable resources is forcing mankind to find renewable and sustainable alternatives to petroleum-based products. Biochar for instance has served as an adaptable renewable raw material for various purposes because of the versatility of qualities it possesses. Some modern high-performance applications demand some specific properties of biochar. Nevertheless, biochar from different feedstock shows promising signs, as its properties can be modified by process conditions or through chemical treatment. (Schmidt, 2012)

Biochar can be produced from almost any kind of plant-based material, by using pyrolysis techniques for example. When organic material is pyrolyzed, all volatile compounds are burned, and carbon is left. This carbon is called biochar. Such plant-based materials are low-cost, widely available and renewable, they could reduce dependence on oil, and have favorable impacts on rural economies (Schmidt, 2012).

Polyurethanes, on the other hand, have been widely used in various applications for many decades. Examples of the most common polyurethane applications are in furniture, thermal insulation, footwear, straps, and coatings (Marktool, 2015). The properties of polyurethane polymers can be modified by using different amounts of soft and hard segments. Polyurethanes are really versatile, and used widely in many products from bathroom sponges to conveying rolls in ore transportation. Polyurethanes are also resilient materials and have good wear properties together with good chemical durability. Polyurethanes are made out of two or more liquid phase chemicals. The main chemicals are polyol and isocyanate. Because the chemicals are liquid, it is easy to cast products with various shapes. Polyurethanes are naturally good insulators (with resistivity of $1.5 \cdot 10^{-12}$ ohms ($\Omega$)), but can be modified into conductive materials. (Lima et al., 2012) Many studies have described the use of polyurethanes with carbon-based additives as conductive composite materials. (Donnet et al., 1993, Fenguli et al., 1999, Nan et al., 2015, Hu et al., 2016)

Insulating materials can be converted into electrically conductive material by increasing the amount of electrically conductive additive in the polymer. This kind of behavior can be modeled using percolation theory. When additive is added to reach a specific point, the composite will have a critical amount of electrically conductive particles and the percolation threshold is achieved. Around this point, the electrical properties of the material change by multiple orders of magnitude. There are various different models for modeling percolation in materials, for example Monte Carlo simulations and the Janzen percolation model (Janzen, 1975). As theory and practice tend to differ from each other, this percolation threshold is measured by the change in conductivity between different additive amounts (Behnam et al., 2007).

Most of the studies done concern carbon black and different kinds of carbon nanotubes as additives, which have promising results with good electrical properties. These kinds of additive are synthetically produced, whereas biochar is a bio-based material. This makes biochar an interesting alternative to these synthetic materials.

The subject of this thesis is how environment-friendly, renewable biochar performs as an additive for electrically conductive polyurethane composites. The polyurethane composites made for this thesis work were soft polyurethanes based on polyurethane and biochar. These composites are studied as sensing coatings for ore transportation. One possible application could be multilayer polyurethane, where the lower layer is electrically conductive. This would make it possible to measure when the polyurethane coating has worn too much. The aim is to study how the biochar content affects the electrical conductivity, wear properties, and hardness of the composite material. These properties were studied with an abrasion tester and by measuring the Shore hardness of the samples. Electrical properties were studied by means of dielectric measurements.

# 2 MATERIALS

## 2.1 Polyurethane

Polyurethanes (PU) are an important class of thermoplastic and thermoset polymers, which are obtained by polycondensation reactions among different polyols, isocyanates, and possible additives. This method leads to a wide variety of polymers with different properties and applications. Mechanical and chemical properties can be engineered by the reaction between polyisocyanates and hydroxyl groups, generating urethane groups. Branching can be obtained by adding previously produced urethane groups. Functionality can be increased when producing branched or cross-linked polymers. Other structural changes can also be made altering the synthetic routes, manufacturing process, and the nature of the monomers. (Oliveira et al., 2012)

Polyurethanes are a special group of heterochain polymers characterized by the following structural unit, which is presented in Figure 1 (Bayer, 1947). In this figure, urethane groups (-NH-COO-) are bonded with hydrocarbon groups (R and R´).

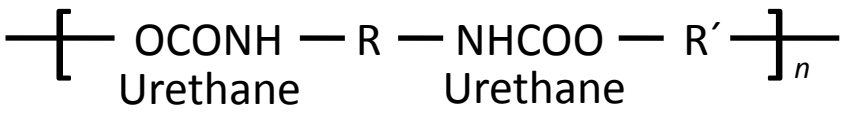


Figure 1. Structural unit of polyurethane (adapted from Ionescu, 2005, p. 1).

The urethane groups, -NH-COO-, are esters of carbamic acid [R-NH-COOH], which is hypothetically unstable, and impossible to obtain under normal conditions (Ulrich, 1996). Urethane groups can be synthetized by various methods with the most important one being the reaction between an isocyanate and an alcohol (Bayer, 1947; Ulrich, 1996). This reaction is exothermic and leads to the formation of polyurethane formation

(Szycher, 1999). It was used for the first time as early as 1849 by Wurtz (Ulrich, 1996). The reaction is shown in Figure 2.

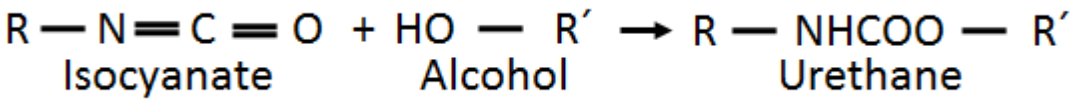


Figure 2. Reaction between isocyanate and alcohol (adapted from Ionescu, 2005, p. 1).

Polyurethanes can be divided into two main categories when considering practicalities and applications: elastic polymers, e.g., flexible foams, elastomers, coatings, adhesives, fibers etc.; and rigid polyurethanes, e.g., rigid polyurethane foams, structural foams, wood substitutes, solid urethanes, etc. This commonly used classification of polyurethanes into elastic and rigid polyurethanes is mainly based on the oligo-polyol structure. (Ionescu, 2005)

### 2.1.1 Polyols

From the point of view of polymer chemistry, polyols are compounds that contain multiple hydroxyl functional groups available for organic reactions. Polyols may also contain for example ester, ether, amide, acrylic, metal, metalloid and other functionalities along with hydroxyl groups. Polyols in polymeric applications are usually polyethers or polyesters. If a polyol has two available hydroxyl groups, it is called a diol, if it has three groups it is called a triol, four groups a tetraol, and so on. (Sharmin and Zafar, 2012)

Polyols, which are used in the manufacturing of polyurethane (PU), can be divided into two groups in terms of structure. The first group is low molecular weight (MW) polyols. Examples of the most commonly used low molecular weight polyols are propylene glycol, ethylene glycol, dipropylene glycol, 1,4-butanediol and glycerol. These polyols

are used in PU manufacturing as chain extenders or crosslinkers, which is why they produce rigid polyurethanes. Chain extenders have two hydroxyl groups/mole, and therefore are termed diols. Crosslinkers have more than two hydroxyl groups/mole, and are termed triols, tetraols etc. The second group is that of high (MW) polyols, which are used to produce flexible polyurethanes. (Ionescu, 2005)

The MW of the oligo-polyols used in polyurethane synthesis varies between 300–10000 Da (meaning g/mol). When referring to low MW polymers (oligomers), the number of hydroxyl groups/molecule of an oligo-polyol is generally in the range of 2–8 OH groups/mol. (Ionescu, 2005)

When making elastic polyurethane, the polyols used have low functionality with around 2–3 OH groups/mol and a high MW of 2000–10000 Da. When using a low MW oligo-polyol of 300–1000 Da with high functionality, a rigid, crosslinked polyurethane of around 3–8 OH groups/mol is produced. When diisocyanate reacts with a high MW diol, for example a polyether or polyester diol with an MW of 2000–4000 Da, it produces very elastic and linear polyurethanes (polyurethane elastomers) (Bruins, 1969). The urethane and urea linkages generate the hard domain or hard segment of a polyurethane elastomer. This is due to the possibility of association with hydrogen bonds. If high MW polyol chains are highly mobile, a soft domain or soft segment is formed. These structures assure the high elasticity of the produced polyurethane elastomer (Figure 3). (Ionesco, 2005)

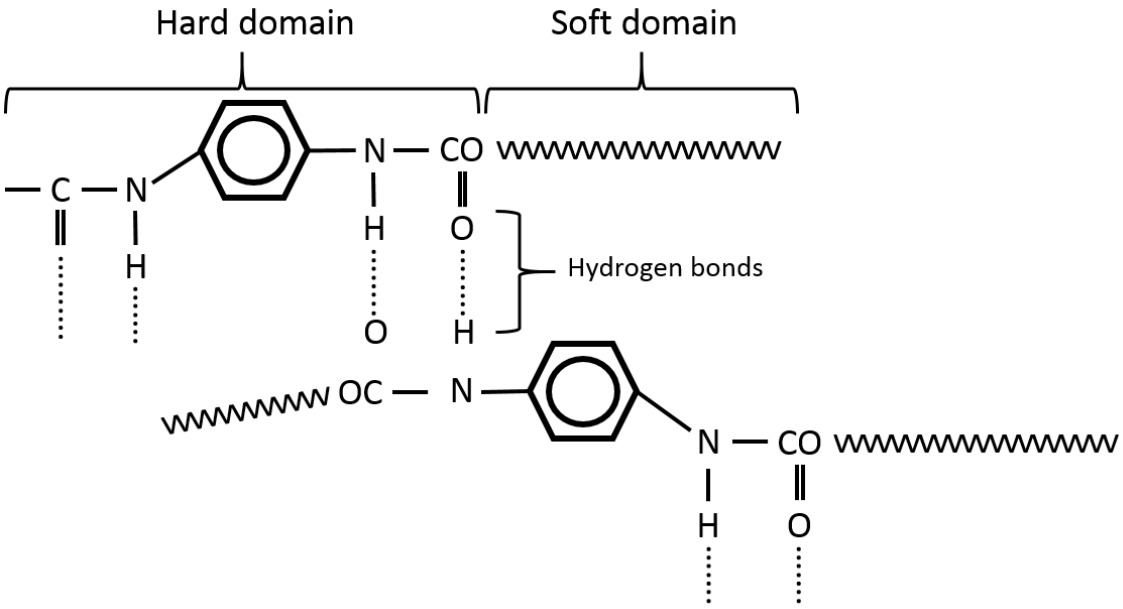


Figure 3. The hard domains and soft domains of polyurethane elastomers (adapted from Ionesco, 2005, p. 7).

When using a polyol with a high MW (3000–6500 Daltons) and low functionality, around 2–3 OH groups/mol, the polyurethane produced will have a less crosslinked structure. Flexible polyurethane foams have this kind of structure. Since it has three OH groups, crosslinking between the urethane bonds will occur. At the same time there is not so much crosslinking, as only 3 bonds can appear, so this kind of polyurethane will be flexible. Because of the crosslinked structure, the MW of this kind of polyurethane is infinite, and only linear polyurethanes have a finite and determinable MW. When producing rigid polyurethanes, polyols with a higher amount of OH groups are used. (Ionescu, 2005)

Usage of low MW polyols (150–1000 Daltons) with high functionalities (around 3–8 OH-groups/mol) leads to a rigid polyurethane structure. When these low MW oligo-polyols of high functionality react with diisocyanate or polyisocyanate, a hard, rigid polyurethane structure is obtained. This kind of high rigidity is a direct consequence of

the high crosslink density of the polyurethane polymer. This is because there are more bonds in the structure, which limit the movement of urethane blocks. (Entelis et al., 1988)

The properties of PU are affected by the degree of crosslinking as well as the molecular weight of polyester polyol (PEP) or polyether polyol (PETP). When using highly branched PEP, processed PU is stiff and has good heat and chemical resistance. If less branched PEP is used, PU will have good flexibility at low temperatures and low chemical resistance. At the same time, low molecular weight polyols produce stiff PU and high molecular weight long chain polyols produce flexible PU. (Sharmin and Zafar, 2012)

Castor oil is one good example of naturally occurring PEP. In addition, the chemical transformation of other vegetable oils results in PEP. Another example of polyols is acrylated polyol (ACP) made by the free radical polymerization of hydroxyl ethyl acrylate/methacrylate with another acrylic. When using ACP, thermal stability is increased in the PU produced. This is one reason why ACP is most often used in coating material applications. Polyols can also be further modified with metal salts (e.g., metal acetates, carboxylates, chlorides), forming metal-containing polyols or hybrid polyols (MHP). When using MHP in PU, thermal stability is good, as is the gloss and anti-microbial quality. (Sharmin and Zafar, 2012)

In this work, a so-called prepolymer is used. Polyurethane prepolymers can be formed by combining an excess of diisocyanate with polyol. The NCO groups of the isocyanate react with polyol OH groups and form a larger complex. The prepolymer reacts like diisocyanate but there are some important differences: prepolymers have higher molecular weight and viscosity, lower isocyanate content by weight and lower vapor pressure than original diisocyanate. Prepolymers are also more stable than diisocyanates. (Prepolymers, 2019)

### 2.1.2 Isocyanates

Isocyanates are essential components of PU synthetization. The isocyanates used are di- or polyfunctional isocyanates containing two or more –NCO groups per molecule. Thanks to their di- or polyfunctional nature, isocyanates work as crosslinkers in PU. There are multiple different isocyanates used in synthetization. They can be aliphatic, cycloaliphatic, polycyclic, or aromatic in nature such as toluene diisocyanate (TDI), methylene diphenyl diisocyanate MDI, xylene diisocyanate (XDI), meta-tetramethyl xylene diisocyanate (TMXDI), 1,6 hexamethylene diisocyanate (HDI), etc. The isocyanate group bears a cumulative double bond sequence such as R-N=C=O, where R is a carbon chain. Aromatic isocyanates are more reactive than aliphatic or cycloaliphatic isocyanates. Some of the most important isocyanates are presented in Figure 4 below. (Sharmin and Zafar, 2012)

As Figure 4 shows, every isocyanate has at least two NCO groups. This tells us that isocyanates work as chain extenders in polyurethanes and various isocyanates have a different effect regarding the properties of the polyurethane produced. These NCO groups react with OH groups as presented in Figure 4.

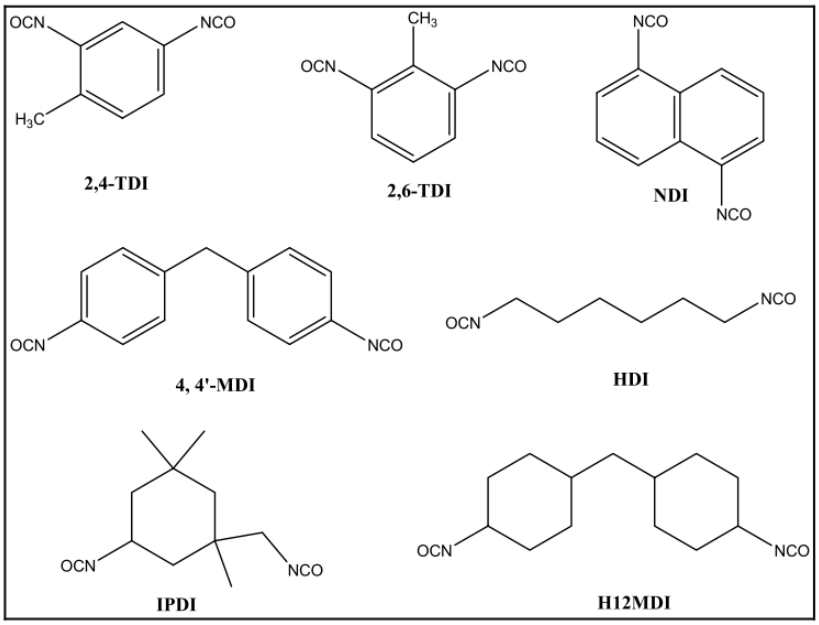


Figure 4. Common isocyanates (adapted from Sharmin and Zafar, 2012, p. 5).

The good reactivity between the isocyanate group and the hydrogen active compounds can be explained by the following resonance structures shown in Figure 5 (Szycher, 1999):

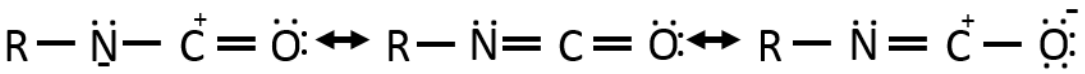

Figure 5. Resonance structure of isocyanate group (adapted from Ionescu, 2005, p. 13).

As Figure 5 shows, the oxygen atom has the highest electron density, while the carbon atom has the lowest. Consequently, the carbon atom has a positive charge, while the oxygen atom has a negative one and the nitrogen atom an intermediate negative charge.

As a result, the reaction of isocyanates with hydrogen active compounds (HXR) is in fact an addition at the carbon–nitrogen double bond. (Szycher, 1999)

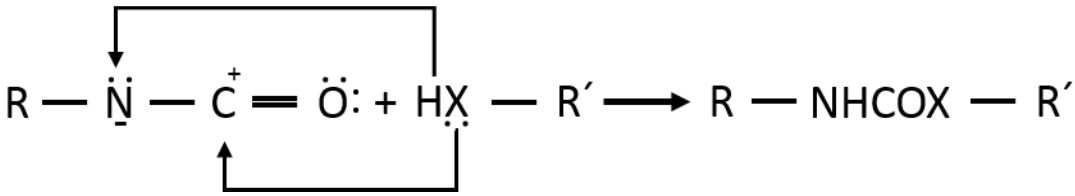


Figure 6. Reaction between isocyanate and hydrogen active compounds (adapted from Ionescu, 2005, p. 13).

The nucleophilic center of active hydrogen compounds (the oxygen atom for hydroxyl groups, or, in the case of amines, the nitrogen atom) attacks the electrophilic carbon atom and the hydrogen is added to the nitrogen atom of the –NCO groups. The reactivity of the –NCO groups is increased by the electron withdrawing groups. The electron donating groups decrease the reactivity against hydrogen active compounds. Aromatic isocyanates are more reactive than aliphatic isocyanates. (Ionescu, 2005)

### 2.1.3 Chain extenders

Chain extenders are reactive, low molecular weight di-functional compounds, for example hydroxylamines, glycols, or diamines. Chain extenders are used to influence the final properties of the PU. The chain extender reacts with the isocyanate to affect the hard/soft segment relationship and therefore the modulus and glass transition temperature of the polymer. The glass transition temperature provides a measure of the polymer's softening point and some indication of the safe upper limit of its working temperature range. (Lees, 2001)

### 2.1.4 Catalyst

As polyol and isocyanate are the main components of PU, some additives are also often used. Most of the time additives are used to control the reaction, modify the reaction conditions, and/or to finish or modify the final product. Additives include catalysts, chain extenders, crosslinkers, additives, moisture scavengers, and colorants. (Sharmin and Zafar, 2012)

The catalysts used in PU production are usually added to promote the reaction at enhanced reaction rates, at lower temperatures, deblocking the blocked isocyanates, and decreasing the deblocking and curing temperatures and times. The most commonly used catalysts are various aliphatic and aromatic amines (e.g., diaminobicyclooctane or DABCO), organometallic compounds (e.g., dibutylin dilaurate, dibutylin diacetate), alkali metal salts of carboxylic acids and phenols (calcium, magnesium, strontium, barium, salts of hexanoic, octanoic, naphthenic, linolenic acid). If the catalyst used is a tertiary amine, its catalytic activity is determined by its structure and basicity. Catalytic activity increases when the basicity is increased, and decreases with steric hindrance of the nitrogen atom of the amine. Metal catalysts are superior to tertiary amines because they are comparatively less volatile and less toxic. Metals catalyze the isocyanate-hydroxyl reaction by means of complex formation with both isocyanate and hydroxyl groups. (Sharmin and Zafar, 2012)

## 2.2 Biochar

The term biochar (BC) was first used around 1998 for the residual of biomass pyrolysis (Bapat and Manahan, 1998). Biochar can also be termed biocarbon or pyrolytic char. Biochar is the solid, carbonaceous residue of the pyrolysis process. Biochar is best known as charcoal (when produced from woody biomass). However, biochar production is not limited to woody biomasses alone as any biological materials can be converted into biochar. Whereas charcoal is mainly used as fuel in heat and power production,

biochar has a wider range of applications. These applications include heat and power production, flue gas cleaning, metallurgical applications, uses in agriculture, animal husbandry and building material, and medical uses (Weber et al., 2018). Biochar is a very diverse material, because its characteristics can be changed by the process parameters and feedstock. Biochar is currently attracting interest because of its large surface area, porosity, adsorptive capabilities, and high fixed carbon levels. (Xie et al., 2014)

As saving the natural environment and renewable natural resources are highly prioritized nowadays, all kinds of bio-based materials are desirable as replacements for oil-based components. Since biochar is made from plant feedstock, it has gained more interest as a material in biocomposites. Using biochar as a additive in composites could help reduce the usage of carbon black (CB) and other synthetic additives (Das et al., 2015). CB is a non-renewable additive, produced from the treatment and processing of hydrocarbons from the oil and gas industry (Wypych, 2009). Although the production of CB is expensive, it is the most widely used additive in industry. CB is also the oldest active additive used. (Fröhlich et al., 2005)

### 2.2.1 Pyrolysis

Pyrolysis is one of the thermochemical conversion methods that occurs in limited or zero oxygen environments (Bridgwater, 2003). The word “pyrolysis” comes from the Greek words *pyro* “fire” and *lysis* “separating”. When biomass is pyrolyzed, a large number of reactions take place, for example dehydration, depolymerization, isomerization, aromatization, decarboxylation, and charring (Lange, 2007). Despite the complexity of the process, it is generally accepted that there are three main stages in biomass pyrolysis. These steps are: (i) initial evaporation of free moisture (dehydration), (ii) primary decomposition, which includes the breakdown of volatile compounds, and (iii) secondary reactions such as cracking and depolymerization, which includes components that divide into biochar and gas. When the gases produced are cooled, heavier gases condense to a liquid state, known as bio-oil. Lighter gases, which remain

as gases, are termed “syngas” (synthesis gas). The pyrolysis process always produces many kinds of products in three phases: solid, liquid, and gas. The relative amount of these products can be affected by the operating conditions (mainly process temperature and residence time) and feed material (Lu et al., 2009). (White et al., 2011)

Biomass can be divided into three main components: cellulose, hemicellulose, and lignin. The amount of these components varies widely in different feedstocks (McKendry, 2001). Each of these components has its own breakdown and decomposition rates and temperatures. Hemicellulose represents a group of polysaccharides with branched chain structures. The decomposition temperature of hemicellulose is 220-315 °C, making it the most reactive of the components. Cellulose is also a polysaccharide, but it is not branched like hemicellulose. Its unbranched structure makes cellulose more thermally stable, and it starts to decompose at temperatures between 280 and 400 °C. Lignin is a complex three-dimensional macromolecule with a variety of different bonds. Because of lignin’s complex structure, decomposition does not occur in a limited temperature range as for cellulose and hemicellulose. The decomposition of lignin occurs all over the temperature range, starting from 200 °C and, depending on the residence time, may go as high as 900 °C to be complete. Since the components partly decompose at the same time, and different feedstocks have a different number of components, it is hard to predict the quality of the product definitively. Figure 10 shows the decomposition temperatures and mass loss rates for each component in thermogravimetric analysis (TGA). (Yang et al., 2007)

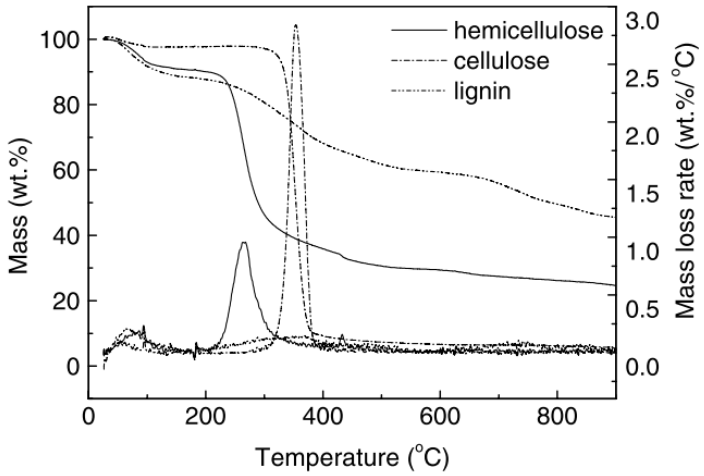


Figure 7. Decomposition of hemicellulose, cellulose, and lignin in TGA (Adapted from Yang et al., 2007, p. 1783).

Pyrolysis is not a new invention, even though the principle of pyrolytic gasification was first used in 1958 at Bell Laboratories, in the United States (Bluechel, 2004). However, the same kind of process has been used for several thousand years to produce charcoal from woody feedstock (Quicker et al., 2016). The Egyptians made pyroligneous acid (wood vinegar, tar, and smoke condensates for bio-oil) for embalming at least 5000 years ago using the principles of pyrolysis (Baumann, 1960).

Fast pyrolysis mostly generates vapors and some aerosols and small amounts of biochar. The most desirable product when using fast pyrolysis is bio-oil, which is produced from cooled and condensed vapors. The bio-oils generated this way have approximately half the heating value of conventional fuel oils. In fast pyrolysis, the temperature increase is 1–100 °C/s up to 450–500 °C and the residence time varies between 1 and 60 s (Cha et al., 2016). The main idea of fast pyrolysis is to use the temperature where thermal cracking occurs, and have as short a residence time as possible to avoid char formation (Mohan et al., 2006). Reported product yields (% of original feedstock mass) are: solids 10-30 %, liquid 50-70 %, gas 5-15 % (Boateng et al., 2010).

Slow pyrolysis maximizes the yield of biochar, and it has been used for thousands of years to produce charcoal. As the name indicates, in slow pyrolysis the temperature rises slowly (1–100 °C/s) up to 350–700 °C and the residence time is several hours (Boateng et al., 2010). A longer vapor residence time allows higher cracking of bio-oil vapors thanks to secondary reactions, and this favors biochar production (Cha et al., 2016). Solid biochar production is increased due to these reactions since vapors re-polymerize on the solid residues and this also has a negative impact on the liquid phase yield and quality (Kan et al., 2016). Reported product yields (% of original feedstock mass) are: solids 15-40 %, liquid 20-55 %, and gas 20-60 % (Boateng et al., 2010).

The principle of flash pyrolysis is basically the same as in fast pyrolysis, yet flash pyrolysis is a more advanced version. The major difference in flash pyrolysis is the residence time of the vapors. The heating rate in flash pyrolysis is more than 1000 °C/s and the temperature range 300–800 °C, whereas the residence time is under one second (Deenik et al., 2010). In flash pyrolysis, the heat and mass transfer along with the chemical kinetics of the reactions and phase transition behavior of the biomass affect the product distribution the most. A high liquid yield is achieved by using a rapid heating rate with high temperature and low vapor residence time (Manoj et al., 2015). Reported product yields (% of original feedstock mass) are: solids 30-40 % and gas 60-70 % (Deenik et al., 2010).

Torrefaction is a mild version of pyrolysis where the temperature is kept between 200–320 °C and the temperature increase rate is less than 1 °C/s. The residence time can be from hours to days (Boateng et al., 2010). In torrefaction, reported product yields (% of original feedstock mass) are: solids 40-90 % and gas 10-60 % (Bridgeman et al., 2008). It has been established that torrefaction increases efficiency when transporting woody biomass in the forest industry. When biomass is torrefacted, it loses moisture and its heating value is increased (Bourgois and Guyonnet, 1988).

### 2.2.2 Biochar composition

As mentioned earlier, the composition of biochar can vary considerably, as it is dependent on the feedstock and process parameters. Different feedstocks have different amounts of the major components, namely cellulose, hemicellulose, lignin, and minerals, which affect the biochar composition. These components have different decomposing temperatures, which is the reason why the feedstock has the biggest influence on the products (Xie et al., 2014). As the biomass components have different decomposition temperatures and rates, the heating rate, process temperatures, and residence times are of secondary importance when talking about effects on the products (Neves et al., 2011). As in every process, one of the most commonly investigated aspects of biochar is the product yield and the product distribution. Since the original composition of the feedstock affects the products a great deal, the parameters can be chosen to achieve the desired products. Figure 7 shows that lignin decomposes much more slowly than cellulose or hemicellulose. Therefore, biochar yields from feedstock with high amounts of lignin are the highest (Pereira et al., 2013). Other factors favorable to biochar yields are long residence time (Lua, Guo, 1998), high pressure (Antal et al., 2000), and any construction to prolong the time that the gasses are in contact with the solids (Wang et al., 2013).

One of the main goals when producing biochar is to change the chemical composition of the material. The most important factor is to increase the carbon content. This can be done by removing functional groups containing oxygen and hydrogen. This is one of the reasons why increasing the reaction temperature gives a higher carbon content and lower content of hydrogen and oxygen. The amount of carbon and oxygen mirror each other: when one increases, the other is reduced. Untreated wood has a typical carbon content of slightly over 50% and oxygen content of a little over 40% (Vassilev et al., 2009). At higher temperatures, a carbon content of 95% may be reached with an oxygen content of less than 5%; when the temperature increases, the amounts of oxygen and carbon approach asymptotically the extreme values of 100% carbon and 0% oxygen. The hydrogen content of wood varies between 5% and 7% and after pyrolysis it

decreases to below 2%. Feedstock and process conditions have only a minor effect on the carbon, oxygen and hydrogen contents of woody biomass, since the content of these elements increases homogenously with rising temperature.

When producing biochar, the process needs to be optimized for solids production. This is achieved by keeping the temperature low and having long processing times. By using low temperature, the amount of vapor and steam is minimized and bio-oil is not produced. Above 400 °C most of the cellulose and hemicellulose has decomposed and the decomposition rate of lignin starts to slow. The carbon content that remains in the structure of the solid after the volatile components have vaporized is referred to as fixed carbon. The fixed carbon content of feedstock affects the yield of biochar significantly. The amount of fixed carbon of raw biomass is normally in the range of 10-30 % and does not change much below the torrefaction range. The amount of fixed carbon is increased to 50-60 % when the torrefaction range (250–350 °C) is reached. A relatively high amount of fixed carbon is achieved at relatively low temperatures. Still, a temperature of over 700 °C is needed to achieve a fixed carbon content of above 90 %. At the same time as the fixed carbon content increases, the volatile matter content decreases. Another issue that raises biochar yields is lower heating rates, which prevent secondary pyrolysis from taking place and thus reduce the amount of thermal cracking. Other parameters affecting the yield of biochar are: vapor residence time, as longer times promote the re-polymerization reactions at the surface of the biochar; particle size, as larger particles produce more biochar; and the height of the reactor bed, for example (Tripathi et al., 2016). (Weber and Quicker, 2018)

Carbon, hydrogen, and oxygen form the majority of biochar, but other elements can also be found, such as chemicals, minerals, and ash. The feedstock has a great impact on the amounts of nitrogen and sulfur present, for example. The concentration of nitrogen and sulfur cannot be increased through pyrolysis, which is why the initial amounts in the feedstock determine the amount of these compounds in biochar (Weber and Quicker, 2018). High nitrogen levels can be found for example in animal waste and sewage

sludge (Tripathi et al., 2016; Xie et al., 2014). As moisture is vaporized during pyrolysis, ash stays in the solid phase and affects the yield of biochar. Consequently, the feedstock has a major effect on the amount of ash in the pyrolysis process. Nevertheless, the ash content appears to rise with temperature, as other material is lost via vaporization and gasification (Weber and Quicker, 2018). Although inorganic materials Si, Ca, K, P, Al, Mg, etc. are not actually ash, they are usually put in the same group, since they do not break down during pyrolysis (Long et al., 2012). As ash can contain many different ions and other contaminants, it can be harmful in some applications. In addition, heavy metals and inorganic toxicants such as copper and arsenic can be found in biochar made from biosolids, pulp water, and other industrial wastes (Srinivasan et al., 2015).

When using a pyrolysis temperature of 700 °C, surface areas of high as 800 $m^2/g$ can be reached (Quicker and Weber, 2016). To put this into perspective, less than 9 g of such biochar would be required to cover a soccer field (7140 $m^2$).

In some applications, there are other requirements apart from a high total surface area. As some gases or liquids are not able to access smaller pores, the amount and size of the pores is a critical feature of biochar. The pores in biochar can be classified into three classes: macropores (pore diameter > 50 nm), mesopores (1–50 nm), and micropores (< 2 nm) (Brewer et al., 2014). As porosity rises when the temperature increases, the total pore volume also increases with rising temperature (Fu et al., 2012). The pore structure of biomass has a large amount of micropores: up to 80% of the total pore volume or surface area (Weber and Quick, 2018).

## 2.3 Electrically conductive composites

A composite material, or in short a composite, is a material which is made from two or more constituent materials with significantly different physical or chemical properties. When these materials are combined, they produce a material with characteristics

different from those of the individual components. Nevertheless, the individual components remain separate and distinct within the finished structure. This is a crucial difference when comparing composites to mixtures or solid solutions. In addition, because of this, most metallic alloys and many ceramics do not belong to the group of composites. A large number of composite materials are composed of just two phases: the first phase is the continuous matrix (resin) and the second phase is the surrounding dispersed reinforcement (fibers and particles). (Callister, 1994)

Polymers in general, with some exceptions such as polypyrrole, polyaniline, and polyacetylene, are inherently insulating materials having an electrical conductivity of the order of $10^{-13}$–$10^{-15}$ S $cm^{-1}$ (Lux, 1993). However, in many cases, there is a demand to have materials with at least some level of electrical conductivity. These composites are called conductive polymer composites (CPC). This kind of composite is obtained by mixing conductive additives, such as carbon black (CB), carbon fibers (CF), carbon nanotubes (CNT), graphene, or any other electrically conductive particles, into the polymer matrix. CPCs have several interesting features, such as high electrical conductivity, light weight, corrosion resistance, relatively low manufacturing costs, and good mechanical properties, for example. (Feller et al., 2003)

Materials with different electrical properties (antistatic, semi-conductive, or conductive) are used in many practical applications. Electro-conductive polymeric materials are often used in heating elements, temperature-dependent resistors and sensors, self-limiting electrical heaters, and switch devices. Antistatic materials are used for the shielding of electronic devices from electromagnetic interference, etc. (Krupa et al., 2007)

### 2.3.1 Electrically conductive additives

It is commonly thought that additives were first added to composite materials in order to decrease the cost (Rothon, 2003). In fact, this is not the case, although sometimes additives are cheaper than the matrix. Nowadays, additives are used to enhance the

properties of the composites or to add new properties. Some of the most commonly used electrically conductive additives are graphite, graphene, CNTs, and carbon black. Carbon black is the most common conductive additive today. It is cheaper than other conductive additives such as metallic powders and glass fibers coated with metals. This is one of the reasons why scientists and material engineers have studied carbon black. The amount of carbon black used is usually between 10–20 weight percent, as the volume fraction can reach as high as 50 %. (Donnet et al., 1993)

As stated earlier, biochar characteristics vary a lot according to the feedstock and process conditions. This means that the characteristics of the additives differ, and the desired properties are different. The polymer in the composite also plays a large role, and it is difficult to predict how the different compositions will perform together. Due to this challenge, the only way to investigate a specific composite material is to create that exact composite and study the properties of the final product.

Biochar on its own has not been studied so much as a composite additive in polyurethanes. According to Nan et al. (2015), biochar has a similar electrical conductive ability to most carbon nanotubes (CNT) and graphene reinforced composites. Other carbon-based materials have been studied more, e.g., CB, carbon nanofibers (CNF), and graphite.

Carbon has been used as an additive material for composites for a long time. Various CNTs, CNFs, CB, graphite, and biochar have been recognized as excellent additives for the production of polymer composites. These components enhance tensile properties, thermal stability, and electrical properties. The high electrical conductivity of these types of polymer composites allows for potential usage in sensors, capacitors, batteries, and many other electrical applications (Nan et al., 2016). The resistivity of neat PU is reported to be $1.5 \cdot 10^{-12}$ ohms (Ω) (Lima et al., 2012). The electrical conductivities of some common carbon additives are shown in Table 1.

Table 1 Electrical conductivity of different additives.

| **Material** | **Electrical conductivity, S/m** | **Reference** |
|---|---|---|
| CNT | $10^6$–$10^7$ | Li et al., 2005 |
| Nanosized steel | $1.35 \cdot 10^6$ | Lewandowska et al., 2009 |
| CNF | 10000 | Al-Saleh and Sundararaj, 2008 |
| Graphene | 7200 | Wang et al., 2008 |
| Carbon black 1300 $m^2g^{-1}$ | 1230 | Pantea et al., 2004 |
| Carbon black 99 $m^2g^{-1}$ | 200 | Pantea et al., 2003 |

The conductivity of graphite depends on several factors, for example the crystallinity, specific surface area, granule size and shape distribution of the material, and on its origin (natural or synthetic). Usually natural graphite has a higher degree of crystallinity and, as a result, it usually has higher conductivity than synthetic graphite (Derieth et al., 2008). According to previous studies, higher conductivity can be achieved when using layered graphite instead of a spherical shape. As spherical particles have a lower specific surface area, it is possible to achieve a higher degree of filling and better processability than when using layered materials. (Shen et al., 2008)

Carbon black has a high specific surface area, up to 1300 $m^2g^{-1}$, and therefore it can be added to the material in smaller amounts. The specific surface area can vary greatly between different kinds of carbon black, and particles with a higher specific area are sufficient to achieve the percolation threshold. The addition of carbon black not only makes the composite more conductive, it also affects the mechanical properties. It may increase the Shore hardness and flexural strength as well as the flexural modulus. (Pantea et al., 2003)

Carbon nanotubes are allotropes of carbon with a cylindrical nanostructure. Carbon nanotubes have exceptional strength and stiffness when compared to any other material, approximately 100 times greater than steel of the same diameter. One special feature of these nanotubes is that they can be constructed with a length to diameter ratio of 132 million to 1. This is also significantly higher than any other material. (Wang et al., 2009) In theory, nanotubes are able to carry an electric current density of $4 \cdot 10^9$ A/cm$^2$, which is 1000 times greater than metals such as copper (Javey et al., 2004). This is because, unlike in metals, in carbon nanotubes the electrons do not need to collide with the atoms. When electrons travel through a carbon nanotube, they travel under the rules of quantum mechanics. This means that electrons go straight through the carbon nanotube material. (Understanding Nano, 2018)

### 2.3.2 Electrically conductive polyurethane composites

When considering conductive materials and their properties, one important property is the electrical percolation threshold. In this phenomenon, conductivity rises by several orders of magnitude when the additive used achieves a specific concentration in the composite. This concentration is different in each composite-additive mix. This phenomenon can be explained by the particle size and concentration in the matrix. When the concentration is low and the additive is dispersed homogenously as small particles, the particles are not able to touch each other in the matrix. When the additive concentration rises, agglomerates are formed which grow until they achieve a size where they start to come into contact with each other. When the particles start to contact, they form a 1-, 2-, or 3-dimensional network. As a result, conductivity increases significantly, and is stabilized for a higher additive concentration. (Lux, 1993)

In classic percolation theories, it is said that the threshold is achieved by the formation of conductive pathways inside the polymer matrix in the form of uninterrupted clusters of conductive additive. At the same time, some other studies indicate the importance of considering quantum effects, such as electronic tunneling between neighboring

particles, in order to explain the electrical percolation threshold, in addition to conductivity. (Vigolo et al., 1999)

The percolation threshold is an important factor when transforming an insulator into a conductor, and it can be calculated. The properties which affect the percolation threshold include particle size, specific area, and particle shape. One of the most commonly used models for the model percolation threshold is the model developed by Janzen (Janzen, 1975). The percolation threshold can be calculated using this model with the following equations 1-3. Equation 1 shows how to calculate the volume fraction where the percolation threshold is achieved:

$$Vf_{\text{biochar}} = \frac{1}{1+4\rho_{\text{biochar}}\nu_{\text{biochar}}} \quad \text{(Eq 1)}$$

where

$Vf_{biochar}$ is the volume fraction of the biochar when the percolation threshold is achieved

$\rho_{biochar}$ is the density of the biochar

$\nu_{biochar}$ is the volume of dibuthyl phthalate (DBP) absorbed per mass of material.

As the percolation threshold is greatly affected by the specific surface area, the latter should be defined. This value can be calculated by Equation 2 where the particles are considered to be spherical. The average particle size of the additive particles is usually measured by laser diffraction and the biochar density is measured by a pycnometer.

$$S_{A-biochar} = \frac{Surface_{\text{biochar}}}{Volume_{\text{biochar}}\,\rho_{\text{biochar}}} = \frac{3}{radius_{\text{biochar}}\,\rho_{\text{biochar}}} \quad \text{(Eq 2)}$$

where

$S_{A-biochar}$ is the specific surface area of the biochar

$surface_{biochar}$ is the surface area of the biochar

$volume_{biochar}$ is the volume fraction of the biochar

$\rho_{biochar}$ is the density of the biochar

$radius_{biochar}$ is the particle size of the additive particles.

As the biochar DPB value has never been measured, it was assumed to be similar to carbon black with the same surface area. By using this DPB value and density of biochar, it is possible to use the Janzen equation when calculating the necessary volume fraction to achieve the percolation threshold.

The mass fraction of additive in the percolation threshold can be calculated by the following equation 3:

$$Mf\text{biochar} = \frac{Vf\text{biochar}}{Vf\text{biochar} + \frac{\rho_{PU}}{\rho\text{biochar}}(1 - Vf\text{biochar})} \quad \text{(Eq 3)}$$

where

$Mf_{biochar}$ is the mass fraction of the biochar when the percolation threshold is achieved

$Vf_{biochar}$ is the volume fraction of the biochar when the percolation threshold is achieved

$\rho_{PU}$ is the density of the polyurethane

$\rho_{biochar}$ is the density of the biochar

Most polyurethanes have very high resistance to electron passage, greater than $1.5 \cdot 10^{-12}$ Ω (ohm), which makes them excellent insulation materials. However, when mixing polymers with highly conductive additives it is possible to produce conductive composites. These composites have several advantages over traditionally used conducting materials (typically metals), for example corrosion resistivity, weight, design, flexibility, adaptability to application requirements, and cost. (Lima et al., 2012)

Fenguli et al. (1999) studied how the properties of polyurethane changed when CB was used as a additive. They found that CB particles were in the form of aggregates and the percolation threshold was achieved first when using at 20 wt% of CB. However, the crystallinity of the soft segments in the polyurethane decreased although the composite had enough soft segment crystals to fulfil the necessary condition for shape memory properties. The study shows that CB is an effective additive for the PU matrix and does not deteriorate the stable physical cross-linked structure of the polyurethane. This

structure is necessary to store the elastic energy in the processing of shape memory materials. Adding CB to the polyurethane makes it stiffer and this affects the recovery properties, especially for higher amounts of CB. Electrical conductivity increases significantly when higher concentrations of CB are added.

Hu et al. (2016) studied how using two additives together affects electrical conductivity. They prepared thermoplastic polyurethane with CNT and graphene biadditives. They found that the percolation threshold of graphene CNT bifillers was about 0.006 vol% when the CNT content was fixed at 0.255 vol%. This content is lower than when using CNT alone and means that adding graphene lowers the percolation threshold significantly when two different additives were used. According to their study, graphene worked as a "spacer" to separate the entangled CNTs from each other and the CNT worked as a bridge between individual graphene sheets. CNTs exhibit a high aspect ratio ($> 10^3$) and high electrical conductivity, making them an excellent additive for conductive composites. According to the percolation theory, the percolation threshold with CNTs has been reported to range from 0.0025 wt% (Sandler et al., 2003) to several wt% (Li et al., 2007).

# 3 CHARACTERIZATION METHODS

When considering the effectiveness of a additive, it is important to look at some key characteristics and their effect on polymer-additive adhesion. A high surface area allows increased adsorption of polymer into the additive, which can increase the interaction between these materials. The tensile strength, yield stress, and fractional resistance of the final product can be improved with increased pore adsorption, although in some situations this may lead to an overly brittle and stiff material (DeArmitt, 2011). One of the most important aspects to control is the particle size of the additive (Peterson, 2012). As smaller particles have a higher total available surface area per volume, this can also allow tighter packing of the additive in the material (Murphy, 2001). Small particles may also raise some problems, as small particles increase the viscosity of the blend and can form aggregates, which act as fracture initiation sites. When it comes to large particles, they can de-bond from the polymer under stress load and act as flaws (Peterson, 2012). One characteristic is also the shape of the additive, as this has the greatest effect on the packing of the material. Additive come in different shapes, and the aspect ratio, i.e., the ratio of length to diameter, is usually the only defining characteristic (Rothon, 2003).

### 3.1.1 BET surface area analysis

When measuring surface area, the most common method is BET analysis, which is named after its inventors Brunauer, Emmet, and Teller. During BET analysis, the sample is exposed to a specific gas atmosphere and the absorbed amount of gas is measured. The most commonly used gas is nitrogen at a temperature of -196.15 °C. The downside of nitrogen is that it has limitations regarding diffusion into micropores (diameter < 2 nm), which is why the surface might be underestimated. An alternative gas is $CO_2$ at a temperature of -0.15 °C; the benefits are a smaller kinetic diameter and higher kinetic energy. Because of these factors, $CO_2$ is able to diffuse more easily into small pores. (Weber and Quick, 2016)

### 3.1.2 Scanning electron microscopy (SEM)

The chemical composition and morphology of composites can be studied efficiently by scanning electron microscopy (SEM). The adhesion between additive and matrix can also be observed from the images. The scanning electron microscope uses a focused beam of high energy electrons to generate a variety of signals at the surface of a solid specimen. The signals, which derive from electron-sample interactions, reveal information about the sample including external morphology, chemical composition, and the crystalline structure and orientation of the materials making up the sample. In most applications, data are collected over a selected area of the surface of the sample, and a 2-dimensional image is generated that displays spatial variations in these properties. SEM can take images ranging from approximately 1 cm to 5 microns in width with a spatial resolution of 50 to 100 nm. SEM is also capable of performing analyses of selected point locations on the sample. This is especially useful in qualitative or semi-quantitative analysis of chemical compositions, crystalline structure, and crystal orientations. (Swapp, 2017)

The accelerated electrons in SEM carry significant amounts of kinetic energy, and this energy is dissipated as a variety of signals produced by electron-sample interactions, when the incident electrons are decelerated in the solid sample. These signals include secondary electrons, which produce SEM images, backscattered electrons, diffracted backscattered electrons used to determine crystal structures and orientations in minerals, photons used for elemental analysis and continuum X-rays, visible light, and heat. (Swapp, 2017)

Energy-dispersive X-ray spectroscopy is used for the elemental analysis or chemical characterization of a sample. This technique relies on the interaction between some source of X-ray excitation and the sample. Its characterization capabilities are due in large part to the fundamental principle that each element has a unique atomic structure, resulting in a unique set of peaks on its electromagnetic emission spectrum. (Goldstein et. al, 2012)

### 3.1.3 Particle size

There is a wide variety of technologies available for determining the particle size distribution of materials. Particles are three-dimensional objects, so three parameters are required: length, breadth, and height. Consequently, it is impossible to describe a particle with only a single number. This is why most sizing techniques assume that the particles in the sample are spherical, as it is then possible to describe them with only one number, the diameter. One of the most widely used techniques is the laser diffraction method; other techniques include dynamic light scatter, sedimentation, image analysis, and acoustic spectroscopy. (ATA, 2010)

Laser diffraction has become the standard method in many industries for characterization and control. Particle analyzers that use this technique rely on the fact that, when particles pass through a laser beam, the sample will scatter light at an angle which is directly related to their size. When the particle size decreases, the observed scattering angle increases logarithmically. Laser diffraction may be used when the particle size in the sample varies between 0.2 and 2000 microns. Measurement is really fast and reliable. This technique can be used when the samples are powders, aerosols, or emulsions. (ATA, 2010)

### 3.1.4 Resistivity and conductivity

Electrical resistivity, also known as specific electrical resistance or volume resistivity, is a fundamental property of a material that quantifies how strongly that material opposes the flow of electric current. When resistivity is low, it indicates that the material readily allows the flow of electric current. The SI unit of electrical resistivity is the ohm meter (Ω•m). A more commonly used variable is electrical conductivity, which is the reciprocal of electrical resistivity, and measures the ability of a material to conduct an electric current (Lowrie, 2007). The SI unit of electrical conductivity is Siemens per meter (S/m). Materials have inner (volume) and outer (surface) resistivity. Whereas volume resistivity represents the material's resistance to leakage current through its

body, surface resistivity measures the resistance to leakage current along the material's surface (Rowe, 2012). When making electrically conductive materials, it is important that the material is electrically conductive. Therefore the resistivity (or conductivity) of the sample is measured.

The most widely used method to measure the resistivity of a film material is by using a four-point probe device. As the name indicates, this method uses four probes. Through the two outer probes, current passes to the sample and at the same time, the potential produced across the two inner probes is measured. The sheet resistance of the sample can be deduced by calculating the ratio of voltage to current. When using the four-probe method, the contact resistance between the probe and material is ignored; however, the geometry of the sample and the configuration of the probe often require correction factors to produce an accurate result (Valdes, 1954). The calculation of correction factors can be avoided by using the dual configuration method. This method requires taking an extra measurement with the probes in a different configuration (Rymaszewski, 1967). Reversing the current applied to the inner probes is also commonly used to eliminate small offset voltages, which are associated with thermoelectric effects (Perloff, 1976).

### 3.1.5 Abrasion test

The Taber abrasion test is designed to compare the wear rate and mass loss of one or more materials or coatings. Normally the Taber abrasion test consists of placing a disk-shaped specimen in constant contact with an abrasive wheel, using a predetermined force for a specified number of cycles to determine wear. There are multiple standards for these tests, but the most common ones are ASTM F4060, ASTM F1978-12, and MIL-A-8625. The Taber abrasion test is a fast and simple way to measure wear resistance and provide sufficient comparable data at low cost. (Castells, 2016)

### 3.1.6 Hardness

When measuring the hardness of plastics, the most commonly used methods are the Shore (Durometer) test or Rockwell hardness test. When measuring rubbers/elastomers, the Shore hardness method is preferred. The Shore method has 12 different scales, but those most commonly used are Shore A and Shore D. The Shore A scale is used to measure "softer" rubbers, and Shore D is used when "harder" materials are measured. (Matweb, 2018) In Figure 8, some examples of Shore values are shown (adapted from smooth-on.com).

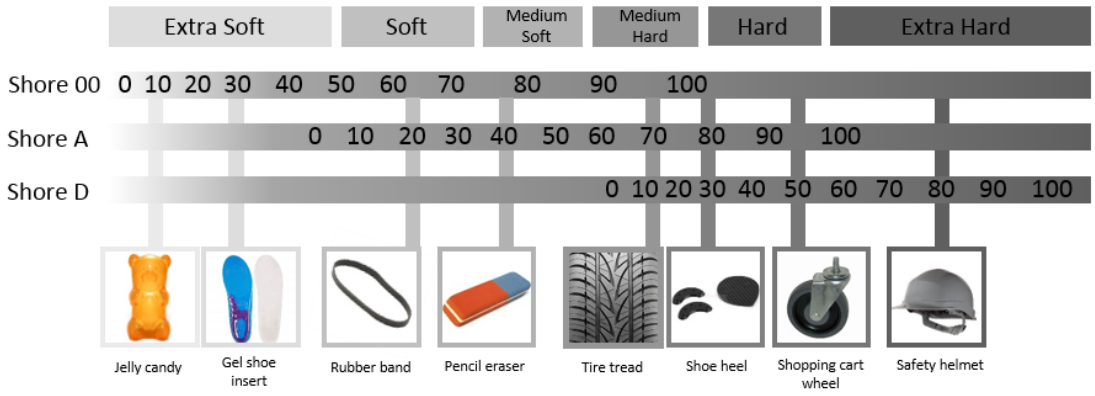


Figure 8. Shore values of some materials (smooth-on.com).

Shore hardness or durometer hardness is measured with an apparatus known as a durometer. The hardness value is determined by the penetration of the durometer indenter foot into the sample. Because rubbers and plastics are resilient materials, the indentation reading may change over time. As a result, the indentation time is sometimes reported along with the hardness number. (Matweb, 2018)

Shore hardness gives the relative resistance to indentation of various grades of polymers. However, the test does not serve well as a predictor of other properties such

as strength or resistance to scratches, abrasion, or wear. Therefore this method should not be used alone for product design specifications. (Matweb, 2018)

### 3.1.7 Porosity measurement

The porosity of the samples was calculated using Equation 4 below. The volume of the sample was calculated according to the measurements of the composite sample. Dimensions were measured using a caliper with a digital screen. The weight of the sample was measured with a semi-micro balance.

$$\varphi = 1 - \frac{\rho_{measured}}{\rho_{calculated}} \quad \text{(Eq 4)}$$

where

φ is the porosity

$\rho_{measured}$ is the measured real density of the composite

$\rho_{calculated}$ is the calculated density of the composite.

### 3.1.8 Raman spectroscopy

Raman spectroscopy is a spectroscopic technique based on the inelastic scattering of monochromatic light, usually from a laser source. Inelastic scattering means that the frequency of photons in monochromatic light changes upon interaction with a sample. The photons of the laser light are absorbed by the sample and then re-emitted. The frequency of the re-emitted protons is shifted up or down when compared to the original monochromatic frequency. This shift is called the Raman effect, and it provides information about the vibrational, rotational, and other low frequency transitions in molecules. Samples in Raman spectroscopy can be in solid, liquid, or gaseous form. (Princeton Instruments, 2018)

# 4 MATERIALS AND METHODS

## 4.1 Materials

### 4.1.1 Polyurethane

The polyurethane used was a two-component polyether polyurethane. The components of the urethane were Adiprene LF 950A and Ethacure 300, and were provided by Ravelast Oy, Kello, Finland. Adiprene LF 950 is a TDI-terminated polyether prepolymer and Ethacure 300 acts as a curative (chain extender) in the polyurethane.

### 4.1.2 Biochar

The biochars used in this study were provided by Noireco Oy, Mikkeli, Finland. They were made from wood using pyrolysis and came from different wood species, namely aspen, birch, and pine. The pyrolysis temperature for the birch was 600 °C and for pine and aspen 370 °C. The biochar samples were delivered as larger particles, almost like barbecue briquettes.

### 4.1.3 Activated carbon

Activated carbon was used as a reference sample. The activated carbon used was ordered from VWR and was provided by Merck Millipore. The CAS number was 7440-44-0.

### 4.1.4 Molds

Two different kinds of Teflon molds were used in this study. Both of the molds were prepared in the workshop of the University of Oulu. The first mold was used to make rectangular polyurethane sheets with a size of 100 x 100 x 4 mm (A in Figure 10 below). The second mold was used to make cylindrical specimens for the abrasion test

with a specimen diameter of 16 mm and height of 13 mm (B in Figure 9 below). Figure 9 shows the molds used in this thesis.

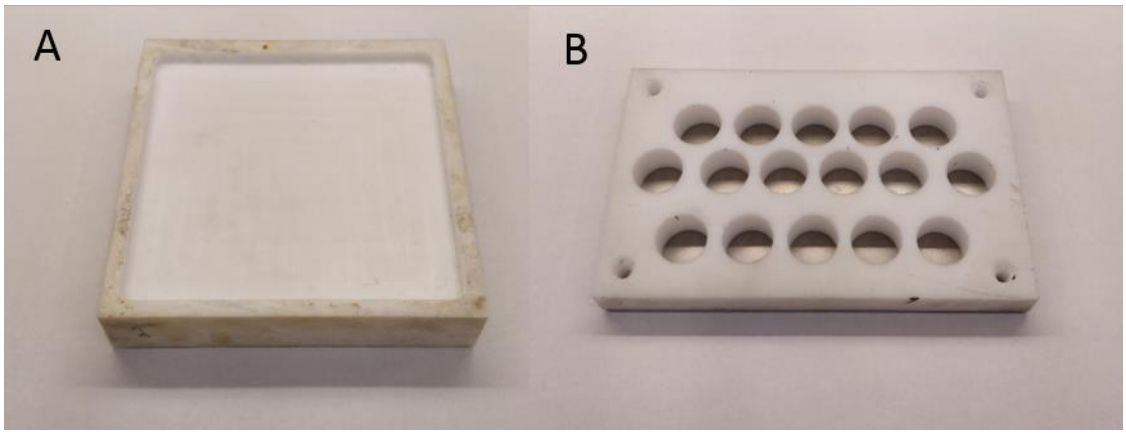


Figure 9. Casting molds for the polyurethane samples. Mold A was used to produce a sample sheet for testing and mold B was used to produce specimens for the abrasion test.

## 4.2 Preparation of biochar powder

Biochar samples were delivered in quite large pieces, so first they were crushed manually using 2 by 4 wood. When all the large pieces had been crushed smaller, crushing was continued with a cross beater mill (SK100, Retsch, Germany). A sieve screen with 500 µm openings was used, meaning that all the particles after this milling were smaller than 500 µm.

After the biochar had been milled once with the SK100, the particle size reduction was continued with a UPZ mill (Hosokawa Alpine, Germany), with pin discs inside. In this mill the following parameters were used: mill speed of 22000 rpm and feed rate of 40 rpm. The biochar was passed through the UPZ mill five (5) times.

After UPZ milling, the sample was mixed with deionized water, and the dry matter content was fixed to 5 wt% for agitated media milling using a 90 AHM mill (Hosokawa Alpine, Germany). The beads used as grinding media in the mill were 3.19 kg of yttrium stabilized zirconium beads (YSZ) with a diameter of 400–600 μm. A speed of 2182 rpm was used, and at this specific speed the peripheral speed was 10 m/s. The aspen and pine biochar samples were milled for 9 hours and the birch biochar sample was milled for 6 hours, after which the formed gel became too thick to go through the mill.

After grinding in the AHM mill, the samples were dried in a freeze-drying machine for one week. It was necessary to use freeze drying as the small particle size of the materials caused them to agglomerate easily. When using freeze-drying, there is less agglomeration when compared to normal drying in an oven.

## 4.3 Preparation of composite samples

The biochar samples were ground using a mortar and pestle before composite preparation, because even the freeze-dried biochar samples contained agglomerates. After grinding, the powder was dried in an oven at 80 °C overnight to be sure that there was no moisture in the powder before mixing with the moisture-sensitive polyurethane.

The polyurethane components, i.e., the prepolymer and the curative, needed to be mixed in the right ratio, in this case 100:14.8 (prepolymer to curative) to obtain the right kind of product. This specific ratio was given by the supplier of the curative. Before use, the chemicals were preheated in an oven for at least 120 min to make them react at the right rate; heating also lowers the viscosity, which affects the mixing properties of the chemicals. The chemicals start to react even at room temperature; heating merely increases the reaction rate. According to the supplier, the curing time when using these components is 30 minutes and the post-cure time 16 hours when the temperature is 100 °C.

After the biochar was dried and the chemicals preheated, they were mixed using a planetary centrifugal vacuum mixer (Thinky, USA). The weighed amounts of biochar, prepolymer, and curative were placed in a mixing cup and mixed for 2 minutes. After mixing, the suspension was poured into a preheated mold and cured in the oven at 80 °C. After 10 minutes, the composite mat was removed from the mold and left in the oven to cure for 16 hours.

A total of 14 different samples were produced, namely PU with 5 wt%, 10 wt%, and 15 wt% of aspen biochar, PU with 5 wt%, 10 wt%, and 15 wt% of birch, PU with 5 wt%, 10 wt%, and 15 wt% of pine, PU with 5 wt%, 10 wt%, 15 wt%, and 20 wt% of activated carbon, and one sample with pure polyurethane. This sample with neat polyurethane is marked zero in the figures. In addition, the author attempted to make a sample with 25 wt% of activated carbon, but it was too viscous to process, as was the sample of 20 wt% of biochar. Examples of mats prepared in this study are shown in Figure 10 below.

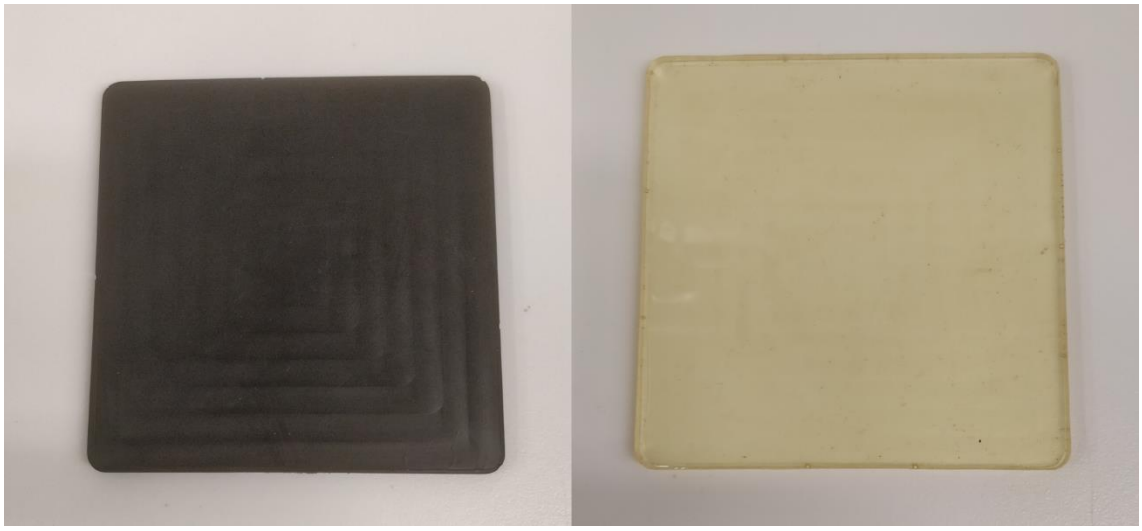

Figure 10. Cast PU/BC with 10 wt% pine biochar composite sheet (left) and neat PU sheet (right) produced in this study.

## Characterization

### 4.3.1 BET surface area analysis

BET surface analysis was conducted using an ASAP 2020 Plus surface area analyzer (Micromeritics Instrument Corporation, Norcross, USA). Biochar samples were degassed at 300 °C for 120 min prior to the $N_2$ adsorption test at -195.8 °C.

### 4.3.2 SEM

The microstructure of biochar samples and biochar polyurethane composites was studied with a field emission scanning electron microscope (FESEM ZEISS Ultra Plus, Carl Zeiss, Germany). The biochar and activated carbon samples were placed on a carbon tab. The composite samples were broken up after being frozen in liquid nitrogen to achieve a fractured surface. After this, the fractured surface of the vertical cross section was sputter- coated with platinum prior to imaging to avoid charging. The microscope was operated using an acceleration voltage of 5 kV.

The chemical composition of the biochar powders was studied using energy-dispersive X-ray spectroscopy (EDX). EDX tests were conducted using a scanning electron microscope (FESEM ZEISS Ultra Plus, Carl Zeiss, Germany) equipped with a silicon drift detector (Oxford X-MaxN 50 $mm^2$, Oxford Instruments, Oxfordshire, U K).

### 4.3.3 Particle size

The particle size of the carbon particles was measured with a Beckman Coulter LS 13 320 particle size analyzer (Beckman Coulter, USA), using the universal liquid

module (ULM) and Tornado dry powder system (TDPS). Samples for ULM particle size analysis were prepared as following: first the samples were dispersed in the disperser solution (Sokolan CP5 5g/l, CP5, BASF, Germany) and then diluted to 0.025 wt% dry matter content with deionized water. After this, the samples were mixed with a magnetic stirrer for 25 minutes and then transferred into an ultrasound bath for 10 minutes. After 10 minutes in the ultrasound bath, the samples were measured. TDPS measures particle size from dry particles, so the particle size using this technique was determined from freeze-dried samples. The sample amount varied between 2 and 3 grams.

### 4.3.4 Raman spectroscopy

Raman spectroscopy was used to study the morphology of the carbon structure of the biochar samples. The analysis was made from 1000–2000 $cm^{-1}$ as the measured bands were approximately between 1300-1700 $cm^{-1}$. The desired bands were the G band, indicating the ordered form of carbon, and the D band, which indicates the unoriented form of carbon. Measurements were made at two machines by using a LabRAM HR800 (Horiba Jobin-Yvon, UK) with a 488nm laser, and the Timegated® Raman Spectrometer. The Timegated device was equipped with a pulsed 532 nm fiber-coupled laser and a CMOS SPAD detector.

### 4.3.5 Resistivity and conductivity

The electrical properties of the composites were measured in the Microelectronics department at Oulu University. Dielectric properties were measured between < 1MHz to 1 GHz range using an inductance, capacitance and resistance (LCR) meter and impedance analyzer. The tester used was a Hewlett Packard 4284A Precision LCR meter, manufactured in the USA. The tester has a self-made sensor, where the sample is set between two electrodes (parallel-plate capacitor). The dimensions of the samples were 25mm x 25mm x 4mm. The distance between electrodes can be adjusted with a

micrometer, and the LCR meter was calibrated before the measurements without a sample. Also, the non-ideality of the device was taken into account in the final results.

### 4.3.6 Abrasion

The wear properties of the composite samples were measured according to the ISO 4649:2010(E) standard. The samples used were prepared in a special dedicated mold. The samples were 16 mm in diameter and from 11 mm to 13 mm in height. In this method, the test piece travels a distance of 40 meters in the sandpaper attached to the drum in the testing equipment. The machine used was a DIN EL-78 abrasion tester from SORACO, Italy. The test was performed at Ravelast, Kello, Oulu. The results are presented as relative volume loss and abrasion resistance index. Equations for calculating the relative volume loss and abrasion resistance index are shown below (equations 5 and 6). The value for the relative volume can be calculated as (ISO 4649:2010(E)):

$$\Delta V_{rel} = \frac{\Delta m_t \Delta m_{const}}{\rho_t \Delta m_r} \quad \text{(Eq 5)}$$

where

$\Delta m_t$ is the mass loss in milligrams of the test rubber test piece

$\Delta m_{const}$ is the defined value of the mass loss in milligrams of the reference compound test piece (200 mg in this case)

$\rho_t$ is the density in milligrams per cubic meter of the test rubber

$\Delta m_r$ is the mass loss in milligrams of the reference compound test piece

The value for the abrasion resistance index can be calculated as (ISO 4649:2010(E)):

$$I_{AR}\frac{\Delta m_r \rho_t}{\Delta m_t \rho_r} x100 \quad \text{(Eq 6)}$$

where

$\Delta m_r$ is the mass loss in milligrams of the reference compound test piece;

$\rho_t$ is the density in milligrams per cubic meter of the test rubber;

$\Delta m_t$ is the mass loss in milligrams of the test rubber test piece;

$\rho_r$ is the density in milligrams per cubic meter of the reference compound.

### 4.3.7 Hardness

The hardness of the samples was tested using a HS100 mechanical Shore A hardness tester manufactured by Innovatest, Netherlands. The tester is pressed against the sample and the result is observed from the scale.

# 5 RESULTS AND DISCUSSION

## 5.1 Biochar characterization

### 5.1.1 Particle size measurements

The particle size of the milled biochars was measured from the gel formed during AHM milling using a Beckman Coulter LS 13 320 particle size analyzer with ULM. The measurement results are shown in Table 2 below. As can be seen, the particle size of pine powder is the smallest. The particle size of birch is smaller than that of aspen, even though it was milled three hours less than aspen or pine. There is also a notable difference between aspen and pine, as the pine particles are more than two times smaller than the aspen particles. The activated carbon that was used has 50 to 100 times larger particles than the biochar samples.

Table 2. Particle sizes as diameter of biochar powders after AHM milling, and activated carbon additive.

| Sample | Mean (µm) | Median (µm) |
|---|---|---|
| Aspen | 0.68 | 0.33 |
| Birch | 0.52 | 0.32 |
| Pine | 0.28 | 0.19 |
| Activated carbon | 34.23 | 28.32 |

Another particle size measurement was made using a Beckman Coulter LS 13 320 analyzer with a Tornado dry powder system. This measurement was done after freeze-drying the biochar powders. The activated carbon samples were not treated in any way. The results are shown in Table 3 below. As the results show, the particle size of the biochars increased considerably during the drying process. The particle size increased 100-fold when compared to the sizes of particles in the gel. This is because small

particles tend to agglomerate really easily. This is undesirable and diminishes many of the particle characteristics.

Table 3. Particle sizes of dry biochar samples after freeze drying. In addition, the activated carbon used as a reference sample was measured.

| Sample | Mean (µm) | Median (µm) |
|---|---|---|
| Aspen | 63.88 | 40.27 |
| Birch | 20.93 | 13.70 |
| Pine | 73.59 | 52.50 |
| Activated carbon | 42.62 | 24.55 |

### 5.1.2 BET

In Table 4 it can be seen that the birch biochar has a much greater surface area than the aspen or pine biochar samples. The reason for this may be that the pyrolysis temperature of birch biochar was higher (600 °C) than in the pyrolysis made for aspen or pine (370 °C). As mentioned before, temperature has a significant effect on the properties of biochar. Another parameter that affects the surface area is the size of the particles among with the porosity. Usually smaller particles have a larger surface area than bigger particles. When comparing aspen and pine biochar, pine has a smaller particle size but a much bigger pore size. For this reason pine has a smaller surface area than aspen. Pine also has a smaller pore volume than aspen. According to Plötze and Niemz, 2011, the wood species has a major effect on the porosity and pore size of the wood. In their study, the porosity of the wood samples varied from 23.30 % (Macassar ebony) to 69.69 % (Sycamore maple). Moreover, the pore size of the samples varied from 10.2 nm (European boxwood) to 12.4548 µm (Scots pine).

Table 4. BET specific surface area results for biochar samples.

| Sample | Mean diameter of particles (µm) | Specific surface area ($m^2/g$) | Pore volume ($cm^3/g$) | Pore size (nm) |
|---|---|---|---|---|
| Aspen | 63.88 | 397 | 0.47 | 4.66 |
| Birch | 20.93 | 607 | 0.59 | 3.92 |
| Pine | 73.59 | 240 | 0.37 | 6.03 |

### 5.1.3 Percolation threshold

As shown in Table 5 below, there is not much difference in the theoretical/mathematical values of the percolation threshold between the biochar additives. Birch biochar has the highest specific surface area and highest density and therefore its percolation threshold is lower than that of the others. Nevertheless, the amount needed to achieve the percolation threshold is high, when compared for example to graphene, which is 3 wt% (Kim et al., 2010). The references used in Table 5 below are taken from CCBI (CCBI, 2019).

Table 5 shows the theoretical values for the percolation threshold when using biochar as additive.

Table 5. Theoretical percolation thresholds for milled biochar additive.

| Sample | Mean (µm) | Density | Specific surface area ($m^2/g$) | Percola-tion (vol %) | Percola-tion (wt %) | DBP $cm^3/100g$ | Reference CB |
|---|---|---|---|---|---|---|---|
| Aspen | 63.88 | 1.47 | 397 | 14 | 18 | 102 | N330 |
| Birch | 20.93 | 2.10 | 607 | 10 | 16 | 113 | N121 |
| Pine | 73.59 | 1.42 | 240 | 13 | 16 | 121 | N550 |

### 5.1.4 Morphology and elemental composition of biochar

The morphology of biochar particles was studied using FE-SEM. Figure 12 shows images of each biochar sample after UPZ pin mill grinding (mean particle size 10–20 µm). In Figure 11, the A images are of the aspen samples, the B images are of the birch samples, and the C images are of the pine samples.


Figure 11. SEM images of pin-milled biochar samples. A1 and A2 are images of aspen samples, B1 and B2 birch samples, and C1 and C2 pine samples.

As Figure 11 shows, biochar particles are of various sizes, and their shape is fairly quadrangular in all samples after UPZ milling. The images on the left side show a general view of the samples and the right-side images show a more detailed view. There are no differences worthy of mention between the biochar samples, which was to be expected, as all are wood-based biochars having similar particle sizes.

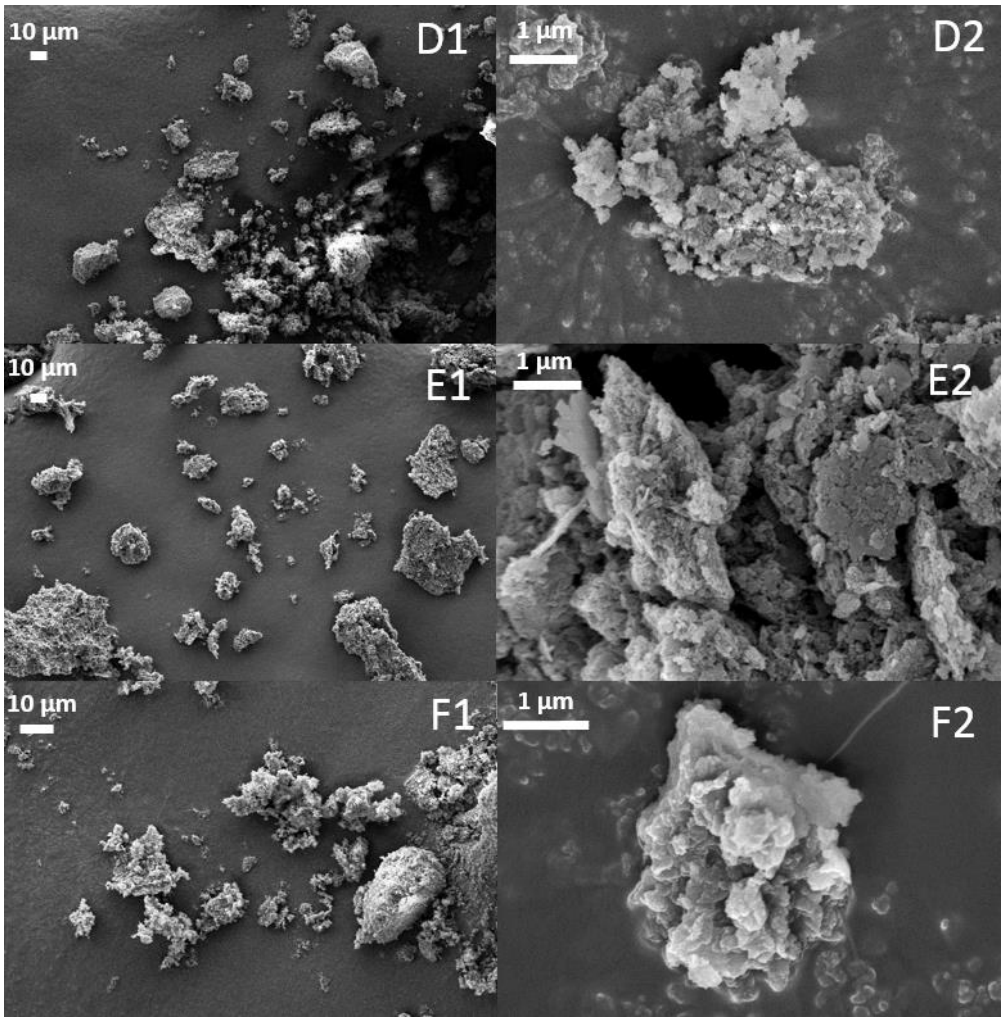


Figure 12. SEM images of AHM-milled biochar. D1 and D2 images are of aspen samples, E1 and E2 birch samples, and F1 and F2 pine samples.

Figure 12 shows biochar samples after AHM mill grinding; the D images are of the aspen samples, E of the birch samples, and F of the pine samples. The images on the left show an overall view of the samples and the images on the right show a more detailed view of the same samples. Figure 16 shows clearly that the biochar particles agglomerate easily. This can be noticed when comparing the particles in the SEM images to the particle size measured. For example, the particle presented in Figure F2 has a diameter of approximately 2.5μm, whereas the particle size determined in particle size analysis was 0.284 μm. In the same image, it can clearly be seen that multiple smaller particles have agglomerated into one bigger particle. The particle size measurements before and after freeze drying also confirm this. This behavior is undesirable because, when particles agglomerate, more particles are needed to achieve the percolation threshold. When comparing different samples (D-F), there is not much difference between them. All the samples exhibit the same kind of behavior.

Elemental analysis of the biochar powders was made by energy-dispersive X-ray spectroscopy. In elemental analysis, different atoms are analyzed and the amounts are shown. In Table 6, the elemental composition of the biochar powders used here is shown.

Table 6. Elemental composition of biochars.

| **Element** | **Aspen** | **Birch** | **Pine** |
|---|---|---|---|
| Carbon | 86 | 89 | 86 |
| Oxygen | 14 | 11 | 14 |

As Table 6 shows, the carbon content of the samples is quite low, between 86 and 89 %. This result was expected, as the pyrolysis temperature was relatively low (370 – 600 °C) and it is known that the carbon content increases as the pyrolysis temperature increases. The desired carbon content would be at least 95 %.

### 5.1.5 Carbon structure

Raman spectroscopy was used to analyze the kind of carbon structures that were represented in the biochar samples. The Raman spectra of the samples are shown in Figure 14.

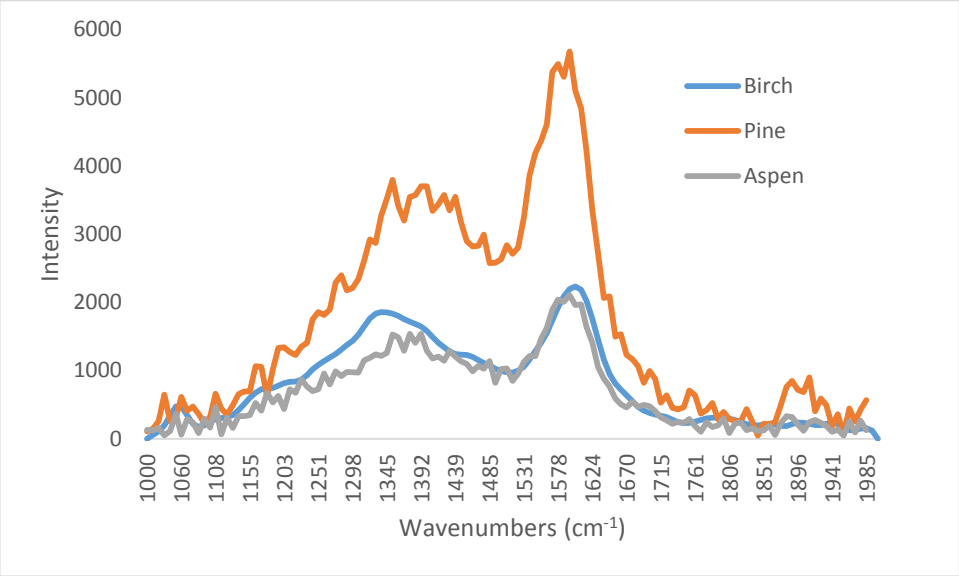


Figure 13. Raman spectra of biochar samples. Samples used in the figure are birch, pine, and aspen.

Different carbon structures give peaks at different wavelengths. The first proper peak in the images is at approximately 1350 $cm^{-1}$ and represents a disoriented structure of carbon. It is known as the D band. The second peak is at approximately 1600 $cm^{-1}$ and represents an oriented form of carbon structure and is called the G band. As higher crystallinity (oriented form) gives better electrical conductive properties (Derieth et al., 2008), it is more desirable than amorphous (disoriented form) carbon. According to the spectra shown in Figure 13, our samples have both crystal and amorphous forms of carbon. Unfortunately, it is not possible to calculate or estimate the ratio between these two forms of carbon from the figures. The images merely show that both types are

represented in our samples. A more important feature in the images is the shape of the peaks. The sharper the peak, the higher the quality of that form of carbon in the sample.

### 5.1.6 Conductivity

The conductivity of the milled samples was measured and the results are listed in Table 6 below. As the results show, only activated carbon has good conductivity. Birch has the best conductivity of the biochar samples, although it is 20 times lower than that of activated carbon. The aspen and pine samples have even lower conductivities than the birch sample. These results show that the temperature used in pyrolysis is not high enough to produce the high quality biochar that is necessary for this application. This can be deduced because birch has much higher conductivity, and is pyrolyzed at higher temperature than the aspen and pine samples.

Table 7. Conductivity of carbon samples.

| Sample | Resistance (Ωm) | Conductivity (S/m) |
|---|---|---|
| Aspen | 11.3 | 0.09 |
| Birch | 3.9 | 0.26 |
| Pine | 11.8 | 0.09 |
| Activated carbon | 0.2 | 5.06 |

## 5.2 Polyurethane-biochar composites

In this chapter, some abbreviated names are used for the samples. The names used for the aspen samples are as follows: PU5ABC, PU10ABC, PU15ABC for aspen samples; PU5BBC, PU10BBC, PU15BBC for birch samples; PU5PBC, PU10PBC, PU15PBC for pine samples and PU5AC, PU10AC, PU15AC, PU20AC, PU25AC for the activated carbon samples. The first two letters show that it is a polyurethane-based composite, the numbers show how many wt% of carbon is added to the composite, and the last letters indicate what kind of carbon is used. When the last letters are ABC, it means that aspen

biochar is used, BBC stands for birch biochar, PBC means pine biochar, and AC stands for activated carbon.

### 5.2.1 Abrasion test

Figure 14 presents the abrasion test specimens before the abrasion test. Figures 15 and 16 show that the wear properties change when carbon additive is added to polyurethane. The addition of activated carbon (AC) has the greatest effect on wear. The addition of biochar has a much smaller effect on wear behavior. When 5 wt% of aspen biochar was added to polyurethane, the abrasion resistance properties were slightly enhanced compared to the pure polyurethane sample.


Figure 14. Abrasion test specimens before testing.

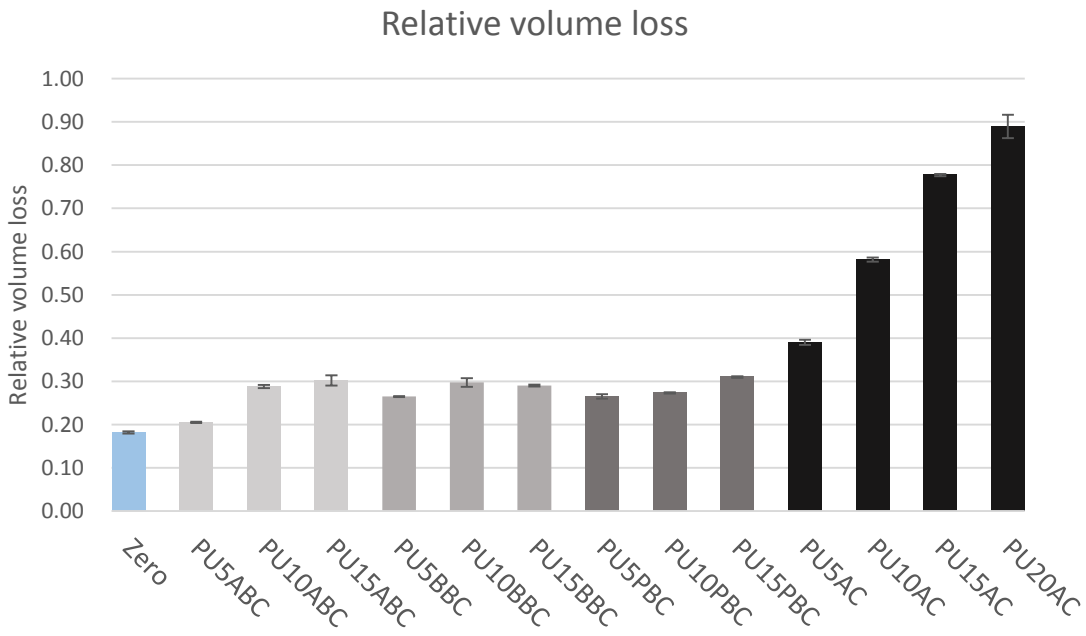


Figure 15. Relative volume loss of the samples in the abrasion test. Zero is a sample made out of polyurethane alone. AC results show the results for composites with different amounts of activated carbon additive. Aspen, birch, and pine results present the results for different biochar samples with different amounts of added additive.

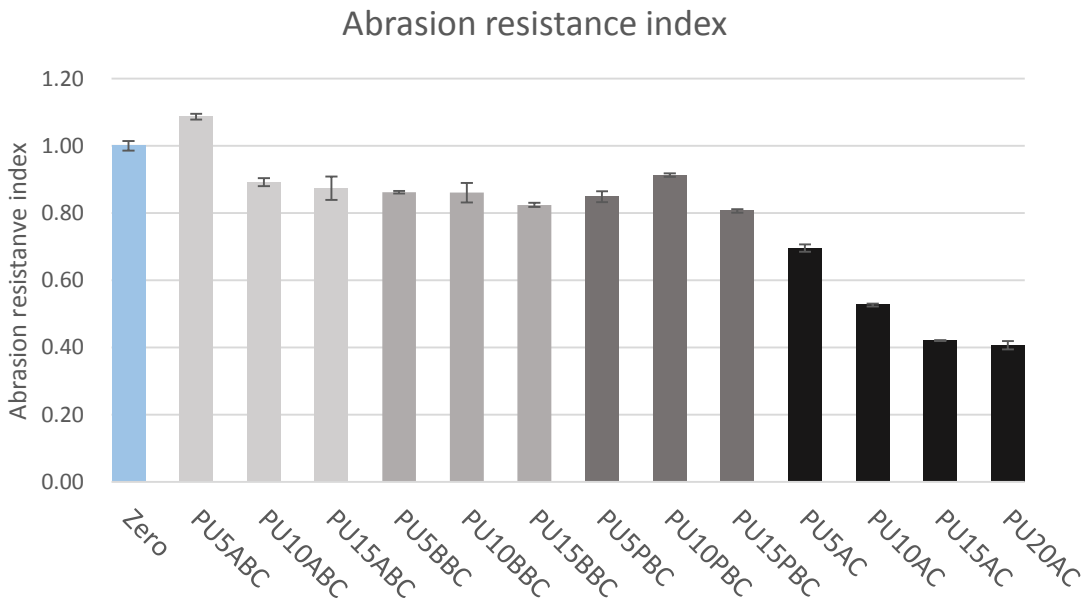


Figure 16. Abrasion resistance index for the PU-BC and PU-AC composites.

When aspen was used as additive, the amount of additive had a significant effect on the relative volume loss. When 5% of aspen was added, the relative volume loss was around 0.2, and when 15% of aspen was added the value was around 0.3. This kind of behavior cannot be seen with the other biochar samples. Birch and pine have relative volume loss values at the same level throughout the line.

### 5.2.2 Structure of abrasion surface

The structure of the abrasion surface was studied by FE-SEM and the results are shown in Figure 17 below. All the samples have the same amount of additive, 15 wt%. Zero images are of the zero sample, and the particles which can be seen in the images are contamination from the composites with biochar. Nevertheless, these images show that the abrasion surface is fairly smooth and there are no bigger particles, as the pure polyurethane is in one phase. Aspen (PU15ABC) and birch (PU15BBC) have fairly similar-looking surfaces and the biochar additive particles are clearly shown. Pine

(PU15PBC) and activated carbon (PU15AC) have similar surface profiles, and more particles can be seen than for aspen or birch. Good adhesion between the biochar additive particles and polyurethane matrix can be seen, as the particles are tightly bonded to the matrix. The activated carbon samples have more loose particles on the surface of the sample, and adhesion between the particles and matrix is not as good as with the biochar powders. Some level of agglomeration can also be seen in the images. Some porosity can also be seen from the images with higher magnification on the right.

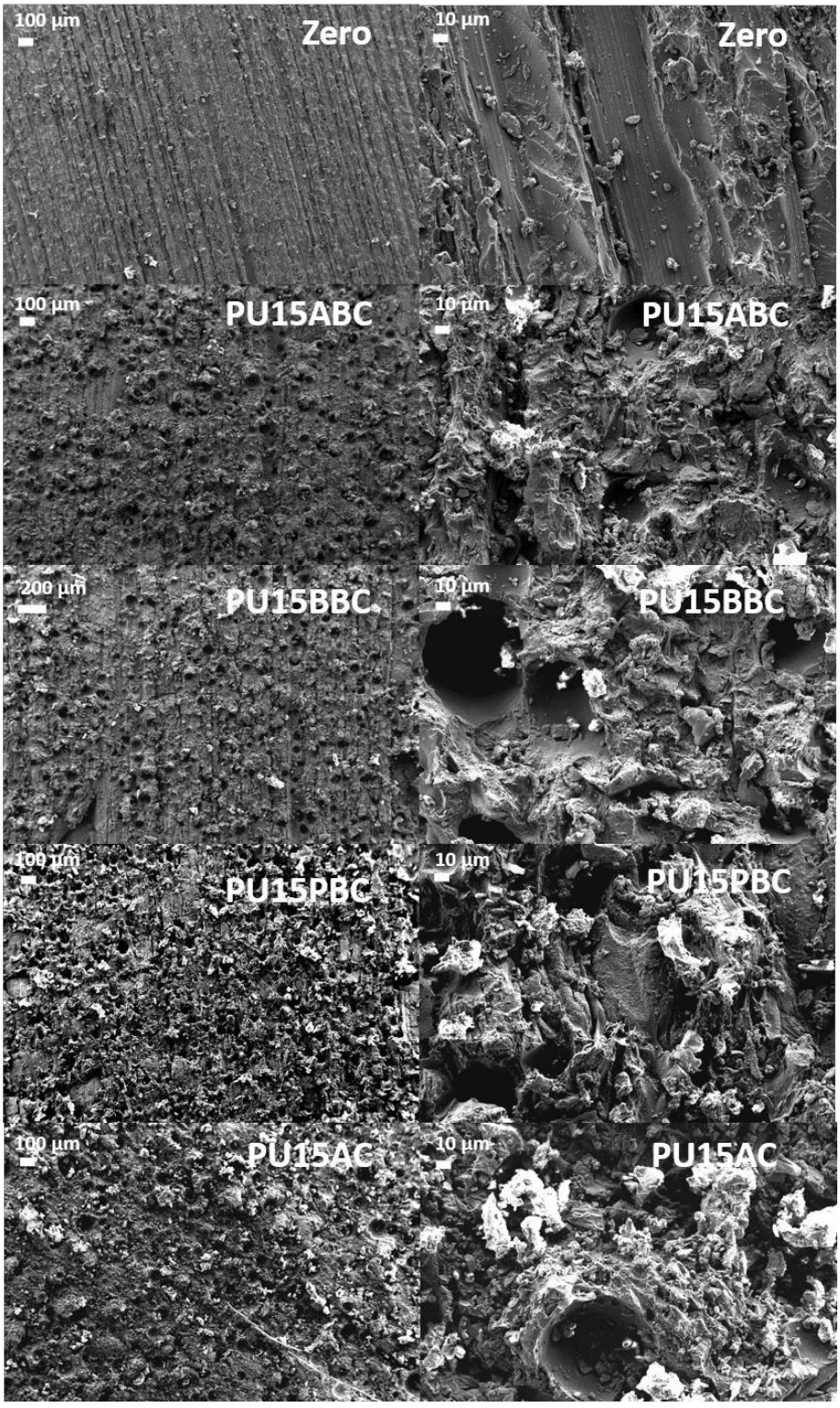


Figure 17. Abrasion surface images of the PU composites. Additive content for all samples is 15 wt%.

### 5.2.3 Hardness

According to the supplier, the Shore A hardness value for polyurethane made of LF-950A and Ethancure 300 is 96. The neat polyurethane sample which was prepared had a Shore A hardness value of 98, which is slightly higher than the value in the literature. The PU-BC and PU-AC composites had Shore A hardness values of between 96 and 98, and the only sample with a value of 96 was 5% activated carbon. All the other samples had hardness values of 97 or 98. The Shore A hardness values of each sample are presented in Table 8 below.

Table 8. Shore A hardness value of carbon samples.

| Sample | 5 wt% carbon | 10 wt% carbon | 15 wt% carbon |
|---|---|---|---|
| Aspen | 98 | 98 | 98 |
| Birch | 98 | 97 | 98 |
| Pine | 97 | 98 | 98 |
| Activated carbon | 96 | 97 | 97 |

### 5.2.4 Fracture surface morphology

Figure 18 presents the fractured surface of the biochar-polyurethane composites: the zero images are of the zero sample, the PU15ABC images are of composites with the aspen additive, the PU10BBC images are of the composite with the birch additive, the PU10PBC image is of the composite with the pine additive, and the PU25AC image is of the composites with the activated carbon additive. Here, again the left-side images show the overall view of the samples and the images on the right show higher magnification images of the same samples.

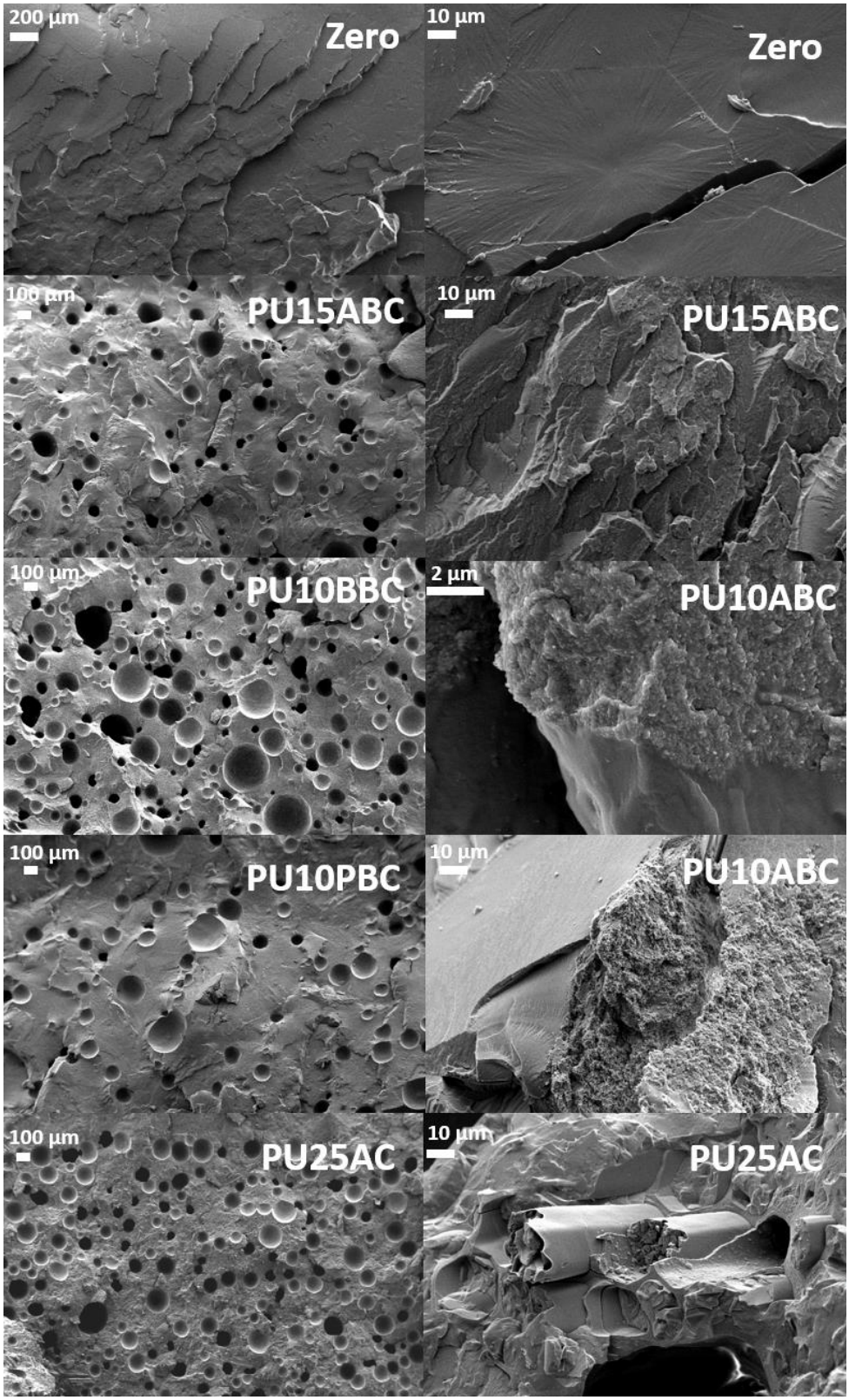


Figure 18. SEM images of composites.

As can be seen in Figure 18 above, all the samples, except the zero sample, have voids. Consequently, it is safe to say that when adding these additives to the polyurethane, voids will form. There might be some unwanted reactions between polyurethane chemicals and carbon additive. On the other hand, additives may contain crystallized water and when the water is mixed with the polyurethane chemicals, it starts to react. This is because all the samples were dried in an oven at 110 °C before usage to ensure their dryness. One possible reason is also that additive particles convey air between the particles and the air is unable to escape during mixing and curing.

All the composites display porosity but there are some differences between the materials. When examining the PU-AC composite, it can be seen that it has the highest number of voids in comparison with the other samples. The size of the voids in this sample is also fairly uniform, with a diameter of approximately 100 μm. This porosity of the PU-AC composite might explain why the abrasion test results were much worse than for the other composites. The composite made of birch has the largest voids (PU10BBC), and the size of the voids varies considerably with the smallest voids being 50 μm and the largest ones 250 μm. The overall structure of the birch-PU composite looks very porous, but it still produced fairly good abrasion test results, as they were just slightly lower than the control sample zero. Composites made of aspen (PU15ABC) and pine (PU10PBC) have a fairly similar structure in the SEM images. These two composites have the smallest number of voids, but the size of the voids varies in the same way as for birch (PU10BBC). Because of the variance between void sizes, it is highly probable that the additives contain some form of water or moisture, which causes these voids. Alternatively, gas was conveyed between the additive particles when the additive was added to the polyurethane.

On the other hand, when looking at the images on the right side, we can see that there is at least good adhesion between the urethane matrix and additive particles. With regard to PU25AC, we can see that the matrix is tightly packed up to the surface of the additive particles. However, this particle exhibits some pull-out phenomena. It can be seen that

there are additive particles protruding from the fractured surface. This means that when the fracture occurred, the polyurethane around the additive particle was pulled out without fracturing the additive particle. This can happen when additive particles are fairly large, as in this case. Please note that not all of the particles are pulled out like this, and many particles were fractured as the matrix was fractured. When viewing the composites made of birch (image PU10BBC) and pine (PU10PBC), we can see that the additive particles have really good adhesion to the polyurethane matrix. Some degree of agglomeration is visible, especially in image PU10ABC.

### 5.2.5 Porosity

As the SEM images of the composites show, all the samples, apart from the zero sample, have voids which affect the composite properties. The porosity of the samples was calculated by using the actual densities, and the calculated densities and results are shown in Figure 19 below. As seen in Figure 19, the porosity increased with increased biochar content, while the activated carbon did not exhibit the same kind of trend. Composites with 15 wt% of BBC showed the highest porosity (14.9%); subsequently the composites with 10 to 20 wt% of AC had the same level of porosity (~4.5%). When comparing different biochars, the addition of pine biochar had the smallest effect on porosity, at 1.5%, and birch showed the greatest effect, and also caused the highest level of porosity in all the samples. When comparing these results to the abrasion test results, there is no clear connection between the two. Even when the porosity of the samples increased, the wear properties stayed at the same level.

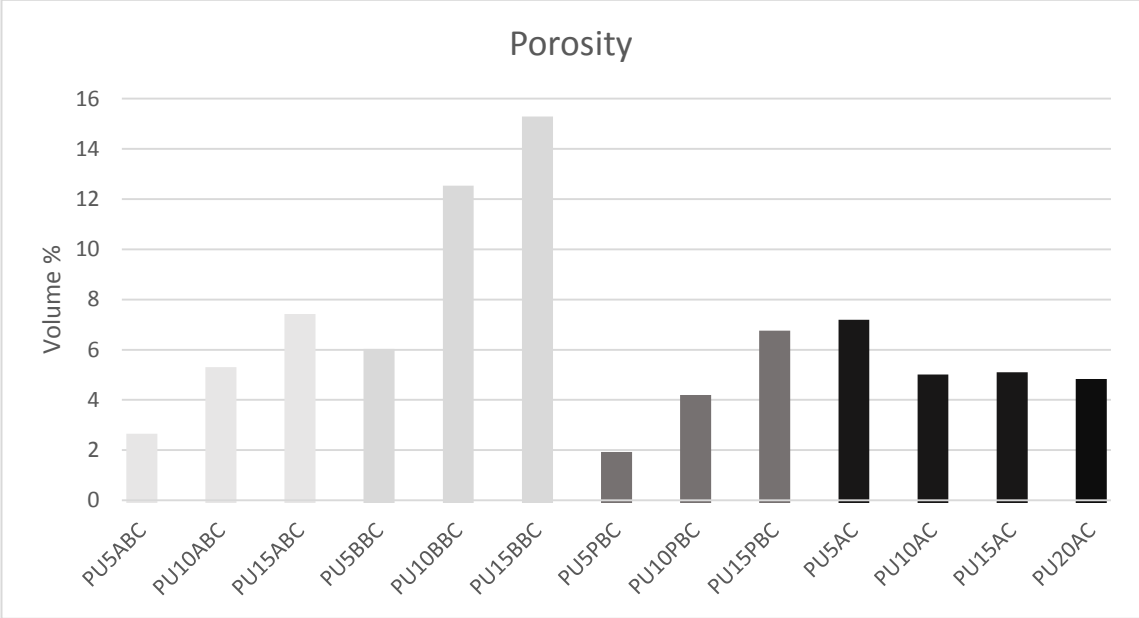


Figure 19. Porosity values for the PU-BC and PU-AC composites.

### 5.2.6 Dielectric properties of composites

The dielectric properties of the polyurethane composites are shown in Figures 20 and 21. In Figure 20, the capacitance of 15 wt% composites is shown. As seen in the figure, the activated carbon sample has the highest values by a large margin. The best biochar is the one made out of birch, which has notably higher values than the aspen or pine biochars. Between aspen and pine there is barely any difference as the values are similarly low. These results can be explained by the pyrolysis temperature of the biochar samples, as birch has a higher pyrolysis temperature (600 °C) than aspen and pine (370 °C). The pyrolysis temperature has an effect on the carbon content and morphology of carbon and also on other properties. Birch also has the highest specific surface area, and therefore the theoretical percolation threshold value is the lowest of the biochars used. Nevertheless, the percolation threshold was not achieved even with birch biochar, because of the low electrical conductivity of the biochar powder. Mechanical percolation should have been achieved, as only around 10 wt% of biochar is required to attain theoretical mechanical percolation.

Figure 21 shows the dielectric loss of the composites. It can be observed here that the birch biochar has a higher dielectric loss at lower frequency than activated carbon. The frequency also has a major impact on the dielectric loss of birch biochar. This kind of behavior cannot be seen with any other sample. Activated carbon and birch have a much higher dielectric loss than the aspen or pine biochars. Nevertheless, the values for aspen, pine, and activated carbon composites are constant throughout the frequency range. According to the dielectric loss measurements, electrical percolation was achieved only with the activated carbon samples. Percolation was achieved somewhere between 20 – 25 wt%. This can be noticed as a "jump" in the values between 20 wt% and 25 wt%.

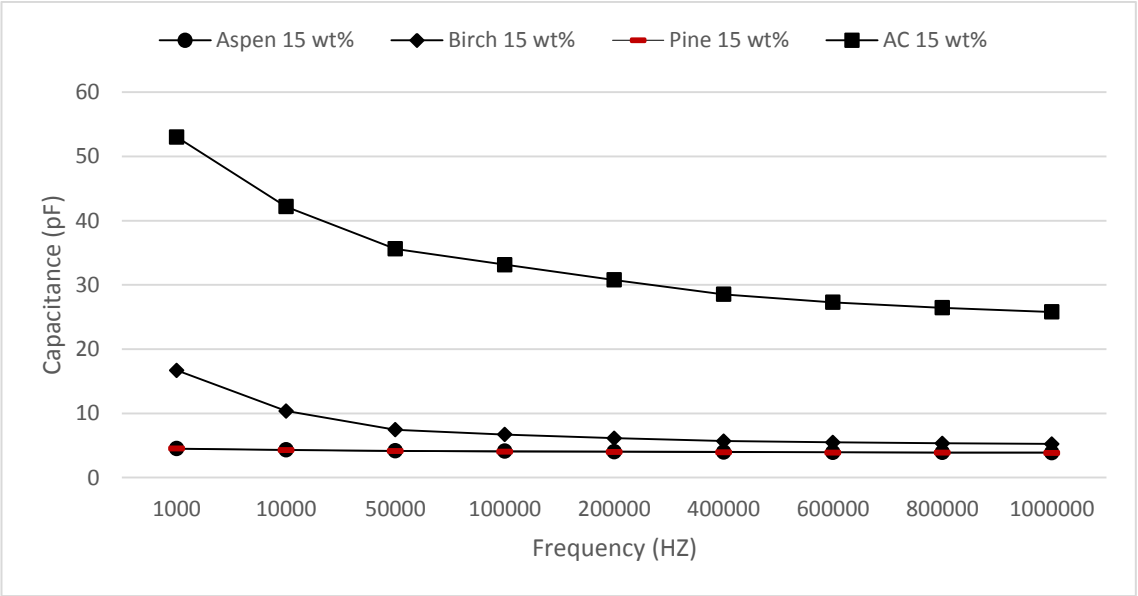


Figure 20. Dielectric properties of BC-PU and AC-PU composites.

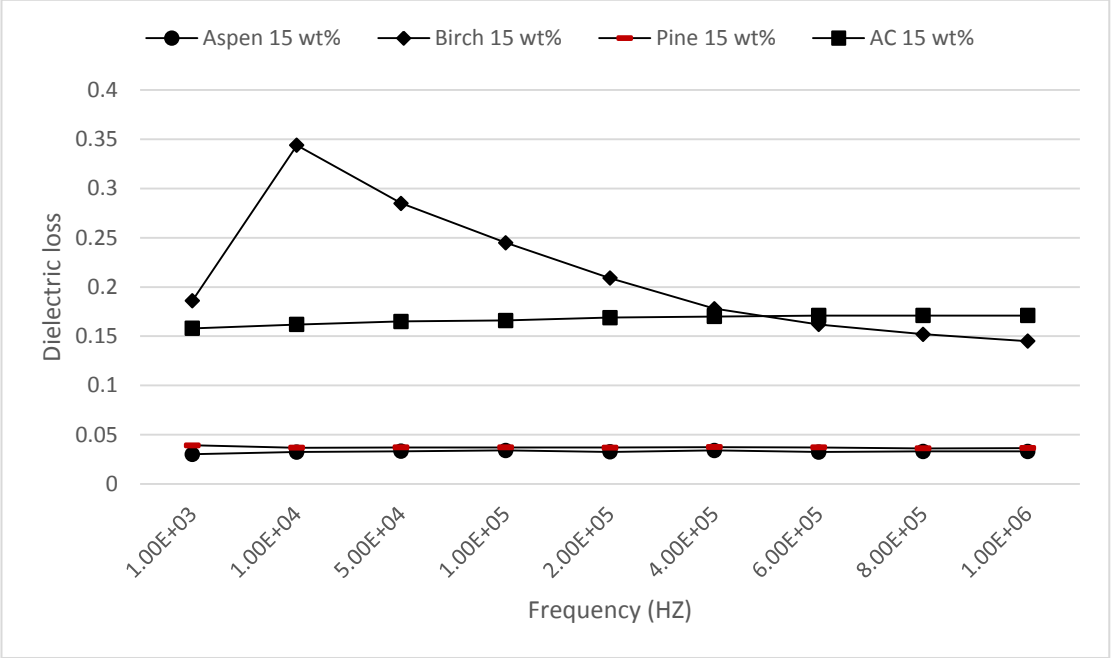


Figure 21. Dielectric loss of polyurethane composites.

## Conclusions

The objective of this study was to prepare polyurethane-biochar composites and study their wear resistance, hardness, and electrical properties. The motivation behind this was the increasing demand to search for renewable bio-based additive materials that could replace the more commonly used additives such as carbon black and graphene. Biochar is a promising candidate because of the numerous favorable properties it possesses. The main findings were that hardness and wear properties did not change much; the void content was fairly high in the composite and the electrical properties were fairly poor.

Composites were successfully prepared by using a mold casting process with an additive amount of 15 wt% or less using biochar powders. The use of activated carbon enabled composites with up to 20 wt% of additive to be made. The addition of biochar had little to no effect on the wear and hardness properties of the composite compared to pure polyurethane. The hardness was the same as for the neat polyurethane, and the wear properties were slightly lower than those of the original polyurethane. Results from the biochar samples were better when compared to the samples with activated carbon. In addition, good adhesion between the biochar particles and polyurethane matrix was achieved according to the SEM images and abrasion test results.

However, the electrical properties of the composites were poor. Even with the largest amounts of biochar additive, the electrical properties were not good enough for applications that require electrically conductive materials. The birch samples had the best electrical properties, and also the abrasion results were good. Electrically conductive composites were achieved when activated carbon was used as an additive, unlike when biochar was used. There are multiple factors which affect this. One of the most important is the low conductivity of the biochar used, due to the low temperatures of the pyrolysis process. Another important factor is the agglomeration of the additive particles. As the SEM images show, particles tend to agglomerate easily into bigger particles which affects the amount of additive needed to achieve the percolation threshold. Also, the particle size measurements, before and after freeze drying the

powders, clearly show the agglomeration of particles. Another factor observed from the SEM images was the porosity of the samples. This has a detrimental effect on the electrical properties, as air or vacuum is a good insulator.

In spite of the lack of electrical conductivity when using biochar powders, biochar-polyurethane composites show promising results. The wear properties and the hardness of the samples were good, and the percolation threshold was achieved when using activated carbon. The electrical properties of biochar powders can be improved by changing the pyrolysis conditions. In the future, different kinds of biochar need to be studied in order to obtain better electrical properties for this composite.

# REFERENCES

ATA Scientific instruments, (2010) An overview of the different particle size measurement techniques. Available at: https://www.atascientific.com.au/overview-particle-size-measurement-techniques/ [6.6.2018].

Aïssa, B., Habib, M. A., Abdul-Hafidh, E. H., Bououdina, M., & Nedil, M. (2015) Carbon nanotubes materials and their related polymer nanocomposites: Frontiers, challenges and strategic priorities. International Journal of Materials Engineering Innovation, 6, 2–3.

Antal MJ, Allen SG, Dai X, Shimizu B, Tam MS, Grønli M. (2000) Attainment of the theoretical yield of carbon from biomass. Industrial & Engineering Chemistry Research 39, 4024-4031.

Bapat, H.D., and S.E. Manahan (1998) Chemchar gasification of hazardous wastes and mixed wastes on a biochar matrix. Abstract of Papers American Chemical Society 215, 008

Baumann, B. (1960) The botanical aspects of ancient Egyptian embalming and burial. Economic Botany 14, 84–104.

O. Bayer (1947) Modern Plastics, 24, 149.

Behnam A, Guo J, Ural A. (2007) Effects of nanotube alignment and measurement direction on percolation in single-wall carbon nanotube films. Journal of Applied Physics 102 (4), 44313. 1–7.

Bluechel Todd (2004) History of pyrolysis. Available at: http://www.balboa-pacific.com/Papers/HistoryOfPyrolysis.pdf [17.04.2018]

Boateng, A.A., C.A. Mullen, N.M. Goldberg, K.B. Hicks, T.E. Devine, I.M. Lima, and J.E. McMurtrey (2010) Sustainable production of bioenergy and biochar from the straw of high-biomass soybean lines via fast pyrolysis. Environmental Progress & Sustainable Energy 29, 175–183.

Boudenne A., Ibos L., Candau Y., Sabu T. (2011) Handbook of Multiphase Polymer Systems, 11, 425-477.

Bourgois, J., and R. Guyonnet. (1988) Characterization and analysis of torrefied wood. Wood Sci. Technol. 22. 143–155.

Brewer CE, Chuang VJ, Masiello CA, Gonnermann H, Gao X, Dugan B, et al. (2014) New approaches to measuring biochar density and porosity. Biomass Bioenergy 66, 176-185.

Bridgeman, T.G., J.M. Jones, I. Shield, and P.T. Williams (2008) Torrefaction of reed canary grass, wheat straw and willow to enhance solid fuel qualities and combustion properties. Fuel 87, 844–856.

Bridgwater, A. V. (2003) Renewable fuels and chemicals by thermal processing of biomass. Chemical Engineering Journal, 91 (2–3), 87–102.

Bridgwater, A. V. (2012) Review of fast pyrolysis of biomass and product upgrading. Biomass and Bioenergy, 38, 68–94.

Bridgwater, A. V., & Peacocke, G.V.G. (2000) Fast pyrolysis processes for biomass. Renewable & Sustainable Energy Reviews, 4, 1–73.

P.F. Bruins, 1969, Polyurethane Technology, Interscience Publishers, London, UK.

Castells Ryan, (2016) Abrasion Testing Explained. Available at: https://www.element.com/nucleus/2016/06/29/abrasion-testing-explained [01.06.2018]

CCBI (2019) Carbon Black, Rubber Carbon Black, Specification of rubber carbon black. Available at: http://www.ccbi.com/ENG_Pages/Product_ENG/P_RCB_ENG.asp [ 24.1.2019]

Cha, J. S., Park, S. H., Jung, S. C., Ryu, C., Jeon, J. K., Shin, M. C., & Park, Y. K. (2016) Production and utilization of biochar: A review. Journal of Industrial and Engineering Chemistry, 40, 1–15.

Das, O., Sarmah, A. K., & Bhattacharyya, D. (2015) A novel approach in organic waste utilization through biochar addition in wood/polypropylene composites. Waste Management, 38 (1), 132–140.

DeArmitt, C. (2011) Functional Fillers for Plastics. In M. Kutz (Ed.), Applied Plastics

Engineering Handbook - Processing and Materials (1st ed., pp. 455–468). Oxford: William Andrew.

Deenik, J.L., T. McClellan, G. Uehara, M.J. Antal, and S. Campbell. (2010) Charcoal volatile matter content influences plant growth and soil nitrogen transformations. Soil Science Society America Journal 74, 1259–1270.

Demirbas A, Arin G (2002) An overview of biomass pyrolysis. Energy Sources, 24 (5), 471–82.

Demirbas, A. (2004) Combustion characteristics of different biomass fuels. Process in Energy and Combustion Science, 30, 219–230.

Derieth, T., Bandlamudi, G., & Beckhaus, P. (2008) Development of highly filled graphite compounds as bipolar plate materials for low and high temperature PEM fuel cells Development of Highly Filled Graphite Compounds as Bipolar Plate Materials for Low and High Temperature PEM Fuel Cells.

Donnet, J-B., Bansal, R.C., and Wang, M-J. (1993) Carbon Black: Science & Technology. New York: Marcel Dekker.

Entelis S.G., Evreinov V.V. and Kuzaev A.I., (1988) Reactive Oligomers, Brill Publishers, Moscow, Russia.

Fadeeva, V. P., Tikhova, V. D., & Nikulicheva, O. N. (2008) Elemental analysis of organic compounds with the use of automated CHNS analyzers. Journal of Analytical Chemistry, 63 (11), 1094–1106.

Fang Q, Chen B, Lin Y, Guan Y. (2014) Aromatic and hydrophobic surfaces of wood-derived biochar enhance perchlorate adsorption via hydrogen bonding to oxygen-containing organic groups. Environ Science Technology 48, 279-288.

Feller, J. F., Chauvelon, P., Linossier, I., & Glouannec, P. (2003) Characterization of electrical and thermal properties of extruded tapes of thermoplastic conductive polymer composites (CPC), 22, 831–837.

Fowler, P. A., Hughes, J. M., & Elias, R. M. (2006) Biocomposites: Technology, environmental credentials and market forces. Journal of the Science of Food and Agriculture.

Fryda, L., & Visser, R. (2015) Biochar for soil improvement: Evaluation of biochar from gasification and slow pyrolysis. Agriculture, 5 (4), 1076–1115.

Fröhlich, J., Niedermeier, W., & Luginsland, H. D. (2005) The effect of filler-filler and filler-elastomer interaction on rubber reinforcement. Composites Part A: Applied Science and Manufacturing, 36 (4), 449–460.

Fu P, Hu S, Xiang J, Sun L, Su S, Wang J. (2012) Evaluation of the porous structure development of chars from pyrolysis of rice straw: effects of pyrolysis temperature and heating rate. Journal of Analytical Applied Pyrolysis.

Garcia-Nunez, J. A., Pelaez-Samaniego, M. R., Garcia-Perez, M. E., Fonts, I., Abrego, J., Westerhof, R. J. M., & Garcia-Perez, M. (2017) Historical Developments of Pyrolysis Reactors: A Review. Energy and Fuels.

Goldstein Joseph, Dale E. Newbury, David C. Joy, Charles E. Lyman, Patrick Echlic, Eric Liftshin, Linda Sawyer, J.R. Michael. (2012) Scanning Electron Microscopy and X-Ray Microanalysis. Springer Science & Business Media.

Gray M., Johnson M.G., Dragila M.I., Kleber M. (2014) Water uptake in biochars: the roles of porosity and hydrophobicity. Biomass Bioenergy 61, 196-205.

Gul V.E. (1996) Structure and properties of conducting polymer composites. Utrecht: VSB BV.

Hill, D.E., Lin, Y., Rao, A.M., Allard, L.F., and Sun, Y.P. (2002) Functionalization of carbon nanotubes with polystyrene. Macromolecules 35, 9466-9471.

IEA Bioenergy (2018) Pyrolysis Reactors, Reactors – Bubbling fluid beds. Available at: http://task34.ieabioenergy.com/pyrolysis-reactors/ [20.4.2018]

Jancar, J. (1998) Structure-property relationships in thermoplastic matrices. Advances in Polymer Sciences, 139, 67–107.

J. Janzen (1975) Journal of Applied Physics, 46, 966–969.

Javey, A., Qi, P., Wang, Q., & Dai, H. (2004) Ten- to 50-nm-long quasi-ballistic carbon nanotube devices obtained without complex lithography.

Kan, T., Strezov, V., & Evans, T. J. (2016) Lignocellulosic biomass pyrolysis: A review of product properties and effects of pyrolysis parameters. Renewable and Sustainable Energy Reviews, 57, 126–1140.

Krupa, I., Mikova, G., & Prokes, J. (2007) POLYMER Electrically conductive composites of polyethylene filled with polyamide particles coated with silver, 43, 2401–2413.

Lange J.P. (2007) Lignocellulose conversion: an introduction to chemistry, process and economics. Biofuel Bioprod. Biorefin., 1, 39–48.

Lees Brian (2001) Polyurethanes – What Goes Into PUS? Available at: https://www.azom.com/article.aspx?ArticleID=218 [31.5.2018]

Li, J., Ma, P.C., Chow, W.S., To, C.K., Tang, B.Z. and Kim, J.K. (2007) Correlations between percolation threshold, dispersion state, and aspect ratio of carbon nanotubes, Advanced Functional Materials, 17 (16), 3207–3215

Lima, A. M. F., Castro, V. G. de, Borges, R. S., & Silva, G. G. (2012) Electrical conductivity and thermal properties of functionalized carbon nanotubes/polyurethane composites. Polímeros, 22 (2), 117–124.

Liu, H., Gao, J., Huang, W., Dai, K., Zheng, G., Liu, C., … Guo, Z. (2016) Electrically conductive strain sensing polyurethane nanocomposites with synergistic carbon nanotubes and graphene biofillers. Nanoscale, 8 (26), 12977–12989.

Long J., Song H., Jun X., Sheng S., Lun-Shi S., Kai X., et al. (2012) Release characteristics of alkali and alkaline earth metallic species during biomass pyrolysis and steam gasification process. Bioresource Technology 116, 278-284.

Lowrie W. (2007) Fundamentals of Geophysics. Cambridge University Press. 254–275. ISBN 978-1-139-46595-3.

Lua A.C., Guo J. (1998) Preparation and characterization of chars from oil palm waste. Carbon NY. 36, 1663-1670.

Lu Q., Li W.-Z., Zhu X-F. (2009) Overview of fuel properties of biomass fast pyrolysis oils. Energy Conversion and Management, 50, 1376–1383

Lux F. (1993) Models proposed to explain the electrical conductivity of mixtures made of conductive and insulating materials. Journal of materials science 28, 285-301.

Manoj Tripathi, J.N. Sahu, P. Ganesan (2016) Effect of process parameters on product of biochar from biomass waste through pyrolysis: A review. Renewable and Sustainable Energy Reviews, Elsevier, 55, 467-481.

Manyà, J. J. (2012) Pyrolysis for biochar purposes: A review to establish current knowledge gaps and research needs. Environmental Science and Technology, 46 (15), 7939–7954.

Mark Tool & Rubber (2015) The 6 Most Common Uses of Polyurethane, Mark Tool & Rubber. Available at: https://www.marktool.com/the-6-most-common-uses-of-polyurethane/ [27.9.2018]

Matweb, Shore (Durometer) Hardness Testing of Plastics, Material property data. Available at: http://www.matweb.com/reference/shore-hardness.aspx [17.9.2018]

McKendry (2001) Energy production from biomass (part 1): overview of biomass Elsevier Bioresource Technology.

Mohan D, Pittman C.U., Steele P.H. (2006) Pyrolysis of Wood/Biomass for Bio-oil: a critical review. Energy Fuels 20 (3), 848–889.

Murphy, J. (2001) Modifying specific properties: Mechanical properties — fillers. In Additives for Plastic Handbook (2nd ed., 19–35). Oxford: Elsevier Science Ltd.

Nan, N., DeVallance, D. B., Xie, X., & Wang, J. (2016) The effect of bio-carbon addition on the electrical, mechanical, and thermal properties of polyvinyl alcohol/biochar composites. Journal of Composite Materials, 50(9), 1161–1168.

Nanda, S., Dalai, A. K., Berruti, F., & Kozinski, J. A. (2016) Biochar as an Exceptional Bioresource for Energy, Agronomy, Carbon Sequestration, Activated Carbon and Specialty Materials. Waste and Biomass Valorization, 7, 201–235.

Juliana Barbero de Oliceira, Luis Gustaco Teixeira dos Reis and Felipe Silca Semaan (2012) Polyurethanes in Analytical Chemistry: A Myriad of Applications from Sorbent Foams to conductive Materials and Sensors. Polyurethane: Properties, Structure and Applications, Nova Science Publishers.

Pantea, D., Darmstadt, H., Kaliaguine, S., & Roy, C. (2003) Electrical conductivity of conductive carbon blacks: influence of surface chemistry and topology, 217, 181–193.

Pereira, B. L. C., Carneiro, A. de C. O., Carvalho, A. M. M. L., Colodette, J. L., Oliveira, A. C., & Fontes, M. P. F. (2013). Influence of Chemical Composition of Eucalyptus Wood on Gravimetric Yield and Charcoal Properties. BioResources, 8 (3), 4574–4592. Retrieved from http://ojs.cnr.ncsu.edu/index.php/BioRes/article/view/BioRes_08_3_4574_Pereira_Eucalyptus_Gravimetric_Yield

Peterson, S. C. (2012) Utilization of low-ash biochar to partially replace carbon black in styrene-butadiene rubber composites. Journal of Elastomers and Plastics, 45 (5), 487–497.

Plötze, M. and Niemz, P. (2011) Porosity and pore size distribution of different wood types as determined by mercury instruction porosimetry. European Journal of Wood and Wood Products, 69 (4), 649-657.

Prepolymers (2019) Available at https://ebrary.net/14336/environment/prepolymers [14.1.2019]

Raman spectroscopy Basics, Princeton Instruments, available at: http://web.pdx.edu/~larosaa/Applied_Optics_464-564/Projects_Optics/Raman_Spectrocopy/Raman_Spectroscopy_Basics_PRINCETON-INSTRUMENTS.pdf [10.10.2018]

Qian, K., Kumar, A., Zhang, H., Bellmer, D., & Huhnke, R. (2015) Recent advances in utilization of biochar. Renewable and Sustainable Energy Reviews, 42, 1055–1064.

Quicker P., Biokohle Weber K. (2016) Herstellung, Eigenschaften und Verwendung von Biomassekarbonisaten. Wiesbaden: Springer Vieweg.

Rothon, R. N. (2003) Particulate-Filled Polymer Composites (2nd ed.). Shawbury: Rapra Technology Ltd. Retrieved from https://app.knovel.com/web/toc.v/cid:kpPFPCE001/viewerType:toc/root_slug:particulatefilled- polymer/url_slug:kt0062Q0M1

Rousset, P. (2014) From biomass to fuel, power and chemicals: Brazilian charcoal-based pig iron. Presented at the Department of Aeronautics and Astronautics, National Cheng Kung University, Taiwan, ROC.

Rymaszewski, R. (1967) Empirical method of calibrating a 4-point microarray for measuring thin-film-sheet resistance. Electron. Lett. 3, 57-58.

Sadaka S., Boateng, A.A. (2017) Pyrolysis and Bio Oil. Agriculture and natural resources.

Sandler, J.K.W., Kirk, J.E., Kinloch, I.A., Shaffer, M.S.P. and Windle, A.H. (2003) 'Ultra-low electrical percolation threshold in carbon-nanotube-epoxy composites', Polymer, 44 (19), 5893–5899.

Schmidt, H.-P. (2012) 55 Uses of Biochar. Ithaka Journal, 25, 13–25.

Seboka, Y. Charcoal Production (2009) Opportunities and Barriers for Improving Efficiency and Sustainability. In Bio-carbon Opportunities in Eastern & Southern Africa: Harnessing Carbon Finance To Promote Sustainable Forestry, Agro-Forestry and Bio-Energy; United Nations Development Programme: New York, Chapter 6.

Sharmin, E., & Zafar, F. (2012) Polyurethane : An Introduction, 3–16.

Shaw, M. T. (2012) Introduction. Introduction to Polymer Rheology. Hoboken: John Wiley & Sons, Inc. 1-14.

Ã, S. C., Mu, P., & Runzhang, Y. (2008). The effect of particle size gradation of conductive fillers on the conductivity and the flexural strength of composite bipolar plate, 33, 1035–1039.

Smooth-On, Durometer Shore Hardness Scale. Available at: https://www.smooth-on.com/page/durometer-shore-hardness-scale [28.9.2018]

Srinivasan, P., Sarmah, A. K., Smernik, R., Das, O., Farid, M., & Gao, W. (2015) A feasibility study of agricultural and sewage biomass as biochar, bioenergy and

biocomposite feedstock: Production, characterization and potential applications. Science of the Total Environment, 512–513, 495–505.

Swapp Susan (2017) Geochemical Instrumentation and Analysis, Scanning Electron Microscopy (SEM). Available at: https://serc.carleton.edu/research_education/geochemsheets/techniques/SEM.html [21.5.2018]

Szycher, M. (1999) Szycher's Handbook of Polyurethanes, CRC Press, Boca Raton, FL, USA.

Tripathi, M., Sahu, J. N., & Ganesan, P. (2016) Effect of process parameters on production of biochar from biomass waste through pyrolysis: A review. Renewable and Sustainable Energy Reviews, 55, 467–481.

Ulrich, H. (1996) Chemistry and Technology of Isocyanates, J. Wiley and Sons, Chichester, UK.

UnderstandingNano (2018) Hawk's Perch Technical Writing, available at: https://understandingnano.com/nanotubes-carbon-properties.html [11.1.2019]

Valdes, L.B. (1954) Resistivity measurements on germanium for transistors. Proc. IRE 42, 420–427.

Vassilev S.V., Baxter D., Andersen L.K., Vassileva C.G. (2009) An overview of the chemical composition of biomass. Fuel 89, 913-933.

Vega, J.F., Martinez-Salazar, J., Trujillo, M., Arnal, M.L., Müller, A.J., Bredeau, S., and Dubois, P.H. (2009) "Rheology, processing, tensile properties, and crystallization of polyethylene/carbon nanotube nanocomposites." Macromolecules 42, 4719-4727.

Velmurugan, R. (2012) Composite Materials. Composite Material, 1–8.

Vigolo, B. (1999) An Experimental Approach to the Percolation of Sticky Nanotubes. Science, (August), 920–924.

Wang, X., Li, Q., Xie, J., Jin, Z., Wang, J., Li, Y., Fan, S. (2009) Fabrication of Ultralong and Electrically Uniform Single-Walled Carbon Nanotubes on Clean Substrates 2009, 1–5.

Wang Y., Hu Y., Zhao X., Wang S., Xing G. (2013) Comparisons of biochar properties from wood material and crop residues at different temperatures and residence times. Energy Fuels. 27, 5890-5899 .

Weber, K., & Quicker, P. (2018) Properties of biochar. Fuel, 217, 240–261.

White J.E., Catallo W.J., Legendre B.L. (2011) Biomass pyrolysis kinetics: a comparative critical review with relevant agricultural residue case studies. Journal of Analytical Applied Pyrolysis. 91, 1–33.

Winsley, P. (2007) Biochar and bioenergy production for climate change mitigation. Science And Technology, 64(1), 5–10. Retrieved from http://www.biochar-international.org/images/NZSR64_1_Winsley.pdf

Wypych, G. (2009) Sources of Fillers, Their Chemical Composition, Properties, and Morphology. In the Handbook of Fillers - A Definitive User's Guide and Databook 2nd. edition, 15–61. Toronto: ChemTec Publishing.

Xanthos, M. (2010) Polymers and Polymer Composites. In Functional Fillers for Plastics: Second, updated and enlarged edition 2nd edition, 2–18. Weinheim: Wiley VCH.

Xie, T., Reddy, K. R., Wang, C., Yargicoglu, E., & Spokas, K. (2015) Characteristics and applications of biochar for environmental remediation: A review. Critical Reviews in Environmental Science and Technology, 45, 939–969.

Yang H., Yan R., Chen H., Lee D.H., Zheng C. (2007) Characteristics of hemicellulose, cellulose and lignin pyrolysis. Fuel 86, 1781-1788

Zhao, B., O'Connor, D., Zhang, J., Peng, T., Shen, Z., Tsang, D. C. W., & Hou, D. (2018) Effect of pyrolysis temperature, heating rate, and residence time on rapeseed stem derived biochar. Journal of Cleaner Production, 174, 977-987